

Extracellular polymeric substances mediate the coaggregation of aquatic biofilm-forming bacteria

Niyati Hede^{a, b} and Lidita Khandeparker^{a*}

a CSIR - National Institute of Oceanography, Dona Paula, Goa 403 004, India

b School of Earth, Ocean and Atmospheric Sciences, Goa University,
Taleigao Plateau, Goa, India

*Corresponding author: Dr. Lidita Khandeparker, Principal Scientist

Email address: klidita@nio.org

Tel.: +91(0)832-2450432, fax: +91(0)832-2450615.

Abstract

Coaggregation, a phenomenon contributing to biofilm formation, occurs among biofilm bacteria from different aquatic environments. However, not much is known about molecules involved in aggregation. In this study, freshwater, estuarine, and marine biofilm bacteria were evaluated for aggregation capabilities, and their cell-bound extracellular polymeric substances (CB-EPS), known to play an important role in biofilm formation, were characterized for functional groups, and sugar composition via Fourier-transform infrared spectroscopy and high-pressure liquid chromatography.

Biofilm-forming potential of estuarine and freshwater biofilm bacteria was higher as indicated by their coaggregation scores, attributed to CB-EPS with distinct sugar types, compared to marine. Most of the biofilm bacteria lost their ability to coaggregate after removal of CB-EPS, indicating its importance in coaggregation. Estuarine (*Bacillus indicus*, *Bacillus cereus*), and freshwater (*Exiguobacterium* spp., *Bacillus cereus*) bacterial pairs, retained their aggregation capability probably via expression of lipids and proteins, suggesting their ability to rebuild themselves by expressing specific biomolecules under stressed conditions. A similar expression pattern was observed when these strains were exposed to abrupt salinity-change (environmental stressor), indicating modulation of cell surface chemistry as a strategy to protect biofilm bacteria in harsh conditions. Unravelling role of these biomolecules as cues for settlement of macrofoulers is a step ahead.

Keywords: Bacteria. FT-IR. Carbohydrates. Biomolecules. 16S rRNA sequencing. *Bacillus* spp.

Introduction

The ability of bacterial cells to aggregate or form biofilms is an adaptive process, wherein they cooperate and improve their chances of survival on sensing and responding to environmental stress (de Carvalho et al., 2018). Many studies have reported that the formation of biofilms, whether it is cell-surface or cell-cell interactions, involves different molecules (e.g. lipids, polysaccharides, proteins, nucleic acids, and some other biomolecules), and processes (e.g. coaggregation and quorum sensing) which contribute to the development of biofilms (Rickard et al., 2000; Watnick & Kotler, 2000; Stoodley et al., 2001; Sauer et al., 2002; Purevdorj-Gage et al., 2005; Irie & Parsek, 2008; Jain & Bhosle, 2009; Rumbaugh & Armstrong, 2014; Kviatkovski & Minz, 2015; Dang & Lovell, 2016; Abisado et al., 2018 etc.). Moreover, recent studies have focused on the importance of coaggregation, a form of cell-cell interaction, characterized by highly specific recognition and adherence of potential partners mediated by lectin-saccharide interactions between cell surface molecules, thereby possibly resulting in the formation of biofilms, originating from these pre-formed cell aggregates (Rickard et al., 2000; Rickard et al., 2003; Kragh et al., 2016; Melaugh et al., 2016).

Coaggregation was first reported by Gibbons and Nygaard, between different species of human dental plaque bacteria in the 1970s. It is not a random process but highly specific recognition and adherence of the bacterial cells that employ specific lectins (protein adhesins or carbohydrate moieties) present on their cell surface to recognize partner bacteria (Rickard et al., 2002; Kolenbrander et al., 2006). This process is a key mechanism and phenomenon in the biofilm formation, which also facilitates interaction among different bacterial species in the biofilms (Rickard et al., 2003). These interactions are known to occur between members of the same genus (intra-generic), same species (intra-species) or with different bacteria (inter-species) (Rickard et al., 2002; Katharios-Lanwermyer et al., 2014). Moreover, the coaggregation process along with autoaggregation, viz. self-aggregation or adherence of identical bacteria to one another (Trunk et al., 2018), depends not only on environmental conditions but also on the distinct bacterial species, that attract potential partners through specific molecules either located on their cell surfaces (including polysaccharide content and the expression of adhesins) or associated with external appendages, thus forming an integral part responsible for the development and formation of multispecies biofilms (Ellwood and Tempest, 1972; Rickard et al., 2000; Rickard et al., 2003; Min et al., 2010). So far, this coaggregation process and the molecules involved have been extensively studied with regard to oral biofilms (Gibbons & Nygaard, 1970; Cisar et al., 1979; Kolenbrander et al., 1993; Palmer et al., 2003; Rickard et al., 2003; Ledder et al., 2009) and is also known to occur within several clinical and non-clinical environments (Adav et al., 2008; Basson et al., 2008; Malik et al., 2003; Simões et al.,

2008; Vornhagen et al., 2013; Cheng et al., 2014; Stevens et al., 2015; Kumar et al., 2019). Relatively few studies have been reported on coaggregation between aquatic biofilm bacteria, e.g. in the freshwater biofilms (Buswell et al., 1997; Rickard et al., 2000, 2002) and marine biofilms (Saravanan et al., 2014). These studies have focused on understanding the role of coaggregation in aquatic biofilm development because of its potential to support or hinder colonization, retention of pathogens within biofilms in shear environments, microbial induced corrosion, and biofouling of surfaces (Stewart & Costerton, 2001; Kerr et al., 2003; Min & Rickard 2009; Katharios-Lanwermyer et al., 2014). The importance of bacterial biofilms and associated biopolymers in the settlement of macrofoulers and their implications in biofouling has been well studied (Khandeparker et al., 2002, 2003; Hadfield, 2011; Dobretsov & Rittschof, 2020 and references within). Moreover, the parentally associated biofilms are unique and play an important role in providing important signals for the settlement of marine invertebrate larvae by producing different types of compounds (Wahl et al., 2012; De Gregoris et al., 2012). Although, it is well known that biochemical cues expressed by the microbial aggregates or biofilms play a very important role in aquaculture and the settlement of the macrofouling organisms (Qian et al., 2007; Dobretsov & Rittschof, 2020), little is known about the mechanisms by which the aquatic biofilm-forming bacteria from different environments aggregate. Moreover, the molecules involved in the process and their relevance in the biofilm formation are least studied, and the same was addressed in the present study.

Biofilms present in all the aquatic environments including freshwater ecosystems (e.g. lakes, inland port, rivers) and marine environments (e.g. estuaries, open ocean), are influenced by several environmental factors such as salinity, nutrient levels etc. (Mora-Gómez et al., 2016). The biofilm bacterial composition and microbial communities in these environments differ (Hede & Khandeparker, 2018; Khandeparker et al., 2017). Hence, it is expected that the composition of exopolymers and mechanisms involved in the formation of biofilms by the aquatic biofilm bacteria would also be different. These aquatic biofilm bacteria range from stenohaline bacteria tolerating only a small range of environmental salinities (marine bacteria) to euryhaline ones with their ability to switch from freshwater or saline water (estuarine bacteria), and the freshwater bacteria which cannot tolerate any salinity changes. Among these, the estuarine biofilm-forming bacteria belong to the most dynamic environment, which is influenced by tides and experiences continuous influx of freshwater, resulting in the changes in salinity (Smyth & Elliott, 2016). Since salinity is regarded as an environmental master factor in the distribution of these aquatic organisms and shaping the bacterial community composition (Stratil et al., 2014; Smyth & Elliott, 2016), any changes in salinity due to environmental conditions or anthropogenic inputs may influence their biofilm formation.

Hence, this factor was used in the present investigation to elucidate how the coaggregation capability varies with respect to salinity changes. Such studies are crucial in understanding microbial behaviour and their environmental responses during the key stages of biofilm formation (Dang & Lovell, 2016). Moreover, the cues expressed if altered with changing environmental conditions will be perceived differently, either by supporting or hindering the settlement of the macrofouling organisms.

Taking the above points into consideration, we examined (1) the biofilm-forming potential of the bacterial strains isolated from biofilms developed in different aquatic environments (freshwater, estuarine, and marine habitats), and (2) characterized the cell-bound extracellular polymeric substances (CB-EPS) of chosen biofilm-forming bacterial strains (freshwater, estuarine, marine) for functional groups and sugar composition via Fourier-transform infrared spectroscopy (FT-IR) and high-pressure liquid chromatography (HPLC). The role of cell-bound EPS was then evaluated by assessing the coaggregation potential of these biofilm-forming bacterial strains in the absence of CB-EPS. The bacterial pairs which could retain their aggregation ability even in the absence of CB-EPS were selected, and the aggregates were characterized using FT-IR. It was hypothesized that the ability of these bacterial strains to cope up with other stressor would be more owing to their high coaggregation potential. These bacterial isolates were exposed to one of the important environmental stressor, i.e. abrupt change in salinity, using laboratory experiments. It was expected that the exposure of these biofilm-forming bacteria to salinity stress would either hinder their ability to aggregate or the tolerant bacterial strains might retain their aggregation capability by expressing specific molecules.

Materials and methods

Sampling site and isolation of bacteria from biofilms

The bacteria were isolated from the in situ biofilms developed on glass slides which were deployed for a period of five days in different aquatic environments, namely freshwater (Kolkata Kidderpore dock area- 22° 32.45994' N, 088° 18.95370' E), and marine environment, including estuarine (Mandovi estuary-15° 30' 17.442" N, 73° 49' 56.2392" E, west coast of India), and open ocean (the Arabian Sea, 15° 51.482' N, 072° 43.511' E). The biofilms were then scraped using a sterile cell scraper (BD Biosciences) in 10 ml of 0.85% saline water (prepared using sodium chloride) for freshwater biofilms, and 0.22 µm filtered autoclaved seawater (~35 salinity) for the remaining two biofilms. After sonication (30W for 60 secs), 100µl of the sample was spread plated on Nutrient Agar (NA, Himedia) for freshwater bacteria and Zobell Marine Agar 2216 (ZMA, Himedia) for marine bacteria. In total, twenty-three successfully isolated bacterial strains from these biofilms were

obtained and referred to as freshwater, estuarine and marine biofilm bacteria which were purified, subcultured and maintained at 4 °C.

Experimental design

The summarised methodological flow chart is illustrated in Fig. 1 and the experimental study was divided into two experiments as described below.

Experiment I: Aggregation ability and identification of biofilm-forming bacteria

Biofilm-forming potential using coaggregation assay

The biofilm formation potential of biofilm bacterial strains was assessed using well-established coaggregation assay. The bacterial isolates were cultured in the nutrient broth (NB) and Zobell marine broth 2216 (ZMB) for freshwater and marine/estuarine biofilm bacteria, respectively and kept on the rotary shaker (Remi, India) for 100 rpm at 30°C. The average period of stationary phase for the isolates was found as 48hrs and 72hrs for freshwater bacteria and marine bacteria, respectively. Cultures (50ml) in their respective stationary growth phases were centrifuged at $4500 \times g$ for 20 min and washed twice with phosphate-buffered saline (PBS), pH 7.4 (Sigma-Aldrich). The cell pellets were then resuspended in sterile PBS, and the working stock (bacterial density: 10^9 cells/ml) was used to determine the aggregation properties of the bacterial isolates. Visual coaggregation assay was carried to determine the qualitative analysis of auto-aggregation and coaggregation between the biofilm bacteria as described below.

Visual aggregation assay

The auto-aggregation and coaggregation were carried out in pairwise combinations between the biofilm bacterial isolates as described by Cisar et al., (1979), with slight modifications. Briefly, 1000 μ l of two different strains of bacteria in PBS (bacterial cell density: 10^9 cells/ml) were mixed in a test tube and then incubated at room temperature for 24hrs. After incubation, the scores for the bacterial aggregation were assigned from “0” to “4” as described by Rickard et al., (2002). Based on the 4-point scale, the turbid supernatant of bacterial culture was assigned “0”, whereas “1” for small uniform aggregates in turbid suspension, “2” for easily visible aggregates with turbid suspension, “3” indicated large settled coaggregates leaving some turbidity in the supernatant and “4” depicted large settled coaggregates with clear supernatant. On the other hand, the auto-aggregation or self-aggregation was determined by mixing equal volumes of the same bacterial suspension, incubated at room temperature for 24hrs and scored from “0” to “4” as mentioned above. The bacterial strains showing strong auto-aggregation and coaggregation scores were identified as biofilm-forming bacteria, and ten strains with high biofilm-forming potential were selected for sequencing as well as

characterization of cell-bound EPS. In addition, the aliquots of these coaggregates were lyophilized and desiccated for characterization using Fourier-transform infrared spectroscopy (FT-IR) as described below.

Identification of selected biofilm-forming bacteria using 16S rRNA sequencing

For identification of selected biofilm-forming bacteria, the marine/estuarine and freshwater bacterial colonies were inoculated into ZMB and NB, respectively. They were incubated at 30°C overnight (approximately 18 hrs) in an incubator shaker at 80 rpm. After the incubation period, overnight grown cultures were transferred to 1.5 ml microcentrifuge tubes and centrifuged at $13,000 \times g$ for 5 min to pellet the cells. The genomic DNA was extracted from the bacterial isolates using Thermofisher® Purelink Genomic DNA Mini Kit, according to the manufacturer's instructions and stored at -20°C until further analysis. Further, the bacterial 16S rRNA gene was amplified by PCR in a 50 μl reaction mixture using Platinum® Blue PCR SuperMix (Invitrogen, USA), 0.25 μM of each primer (8F - 5'-AGAGTTTGATCCTGGCTCAG and 1492 R (1) - GGTTACCTTGTTACGACTT) and template. The PCR products were checked by electrophoresis (2% w/v agarose gel) and purified using the GenElute PCR purification kit (Sigma). These purified products were then sequenced (Bioserve Biotechnologies Private Limited Hyderabad, India). The sequencing results obtained were assembled using DNA Baser and aligned using the Basic Local Alignment Search Tool (BLAST) in the National Centre for Biotechnology Information (NCBI) database (www.ncbi.nlm.nih.gov). These sequences have been deposited in the NCBI GenBank under accession numbers from MH429953 to MH429961 and MH620809. Sequences were aligned with Clustal W, and the phylogenetic tree was built by using the MEGA 6.0 software (Tamura et al., 2013).

Experiment II: Importance of cell-bound extracellular polymeric substances (CB-EPS) in the coaggregation process

Isolation and characterization of CB-EPS from selected biofilm-forming bacteria

For the isolation of CB-EPS, the freshwater and estuarine/marine bacteria were cultured in NB and ZMB for 48hrs and 72hrs respectively, i.e. upto the stationary phase. The cultures were then centrifuged at $4500 \times g$ for 20 min, and the cell-bound EPS were extracted using the EDTA (10mM) as described by Tallon et al., (2003). After centrifugation, an aliquot of the EPS was stored at -20°C for the sugar analysis by high-performance liquid chromatography (HPLC). The remaining aliquot of the EPS was lyophilized and desiccated for the analysis of different types of biomolecules by Fourier-transform infrared spectroscopy (FT-IR).

(i) FT-IR analysis of CB-EPS

A pellet was prepared by grinding approximately 1 mg of lyophilized samples and mixed thoroughly with 2.5 mg of potassium bromide (KBr). KBr was used as a background reference. The spectrum was recorded as an average of 20 scans in the mid-infrared (mid-IR) range of 600-4000 cm^{-1} using Fourier-transform infrared spectrophotometer (IR Affinity-1, Shimadzu, Singapore) at a resolution of 4 cm^{-1} .

(ii) Characterization of sugar composition in CB-EPS by high-performance liquid chromatography

The sugar composition of the CB-EPS was analyzed by reverse-phase high-performance liquid chromatography (HPLC, Agilent 1200 series) equipped with a refractive index detector (RID). The sugars were separated isocratically on a Zorbax Carbohydrate column (4.6 mm I.D. x 150 mm, silica particle size 5 μm , Agilent) using acetonitrile: water (85:15) mobile phase at a flow rate of 1.4 ml/min with a column temperature at 30°C for 35 min. The injection volume of 10 μl was used for each sample and run in duplicates. Before running the samples, the column was calibrated with 19 different HPLC grade sugar standards, i.e. mannose, galactose, rhamnose, sucrose, ribose, glucose, fucose, ribose, arabinose, maltose, N-acetyl-D-glucosamine, fructose, xylose, lactose, inositol, cellobiose, mannitol, sorbitol, melibiose, as described by Sahoo & Khandeparker, (2018). Sugars were identified according to their retention times by comparing with sugar standards (ESM_1). The calibration curves were prepared for each sugar by diluting stock solutions (10 mg/ml) at multiple concentrations. HPLC analysis was then performed for all standard solutions, and the peak area against the retention time for each sugar was recorded. Calibration curves were obtained using the software by plotting peak area versus the amount injected (concentration). The determination coefficients (R^2) were >0.99 , indicating a linear relationship between the chromatographic response areas and the concentrations for all the sugars. The calibration table was then created using this data in the Agilent Chemstation data analysis software. Sugars for samples were identified by comparing with retention times of sugar standards and calculated by the data analysis software. Furthermore, the sugar compositions (%) were subjected to NMDS (non-metric multidimensional scaling) to visualize similarities among the bacterial species and confirmed with Analysis of similarity (ANOSIM) test using PRIMER version 6.0 software (Clarke & Warwick, 1994). Also, the similarity percentage (SIMPER) analysis was carried to identify sugars that significantly contributed to the differences among the biofilm types using PRIMER version 6.0 software.

Role of CB-EPS in biofilm formation

A separate coaggregation assay was conducted after the extraction of CB-EPS (using EDTA method as per the protocol described above) for the selected ten bacterial strains with high biofilm-forming potential to identify the role of cell-bound EPS in the formation of coaggregates. After EPS extraction, the bacterial strains were washed using PBS (pH 7.4). Further, pairs of bacterial strains were mixed (1000 μ l of each strain with equal cell density) in a test tube and incubated at room temperature for 24hrs. Subsequently, the score was assigned based on the coaggregation using the 4-point scale, as mentioned earlier. The estuarine and freshwater bacterial pairs which retained their ability to coaggregate even in the absence of CB-EPS were further characterized as described below.

(i) Visualization of coaggregates using epifluorescence microscopy

The coaggregates of selected bacterial pairs were observed by using epifluorescence microscopy (Olympus, Tokyo Japan). The protocol was standardized, wherein 1000 μ l of each strain in the PBS were stained with either DAPI (50 μ g/ml) or SYBR green nucleic acid (1:10000 final concentration). Subsequently, each of the bacterial suspension was incubated at room temperature in the dark for 20 min to allow staining of the cells. After incubation, the cells were centrifuged at maximum speed (13,000 \times g for 5 min) and washed thoroughly with phosphate-buffered saline (pH 7.4) to remove excess stain. Each strain was then resuspended in fresh PBS solution and mixed to allow them to coaggregate. After 1-2hrs, 50 μ l of the coaggregate was taken on a glass slide for microscopic observation of coaggregates using epifluorescence microscopy. Further, the microscopic images of both Fluorescein isothiocyanate (FITC) and DAPI fluorescence image (green and blue combination) were overlaid using cellSens standard imaging software (Olympus, Tokyo Japan) and Image J software (v. 1.52a).

(ii) Scanning electron microscopy (SEM) of coaggregates

The selected coaggregated bacteria were visualized using a scanning electron microscope (SEM), which allows imaging and investigation of surface topographic features. The samples were fixed using 2.5% glutaraldehyde in phosphate-buffered saline (pH 7.4), then subsequently kept in the refrigerator (4° C) for 1h and dehydrated in the ethanol series. After drying, the samples were examined using a Hitachi Tabletop Scanning Electron Microscope (TM3000).

Comparative characterization of freshwater and estuarine bacterial pairs and their coaggregates before (control) and after the extraction of CB-EPS

(i) Characterization of glycoconjugates on coaggregate surfaces using fluorescent markers

The fluorescent markers (lectins) obtained from Sigma-Aldrich were used to identify surface glycoconjugates of the coaggregated bacterial pairs. The specific lectins used were (1) Concanavalin A (Con A) - FITC conjugated lectin to tag D-mannose/D-glucose residues (Strathmann et al., 2002; Guillonneau et al., 2018), (2) Wheat germ agglutinin (WGA) - FITC conjugated lectin to tag N-acetyl-D-glucosamine and sialic acids, and (3) Glycine max (Soybean agglutinin) - TRITC conjugated lectin (SBA) for tagging N-acetyl-D-galactosamine.

The protocol was standardized for this, wherein the coaggregates formed by the selected bacterial strains after mixing them for coaggregation assay (approx. 1-2 hrs) were stained and incubated with DAPI (50 µg/ml) (Himedia) for 15 min in the dark. Subsequently, the coaggregates were rinsed with PBS to remove excess stain. The coaggregates were then stained with one of the fluorescent markers (1 mg/ml) and visualized under an epifluorescence microscope (Olympus, Tokyo Japan). Similarly, the above protocol was repeated on coaggregates formed after the extraction of cell-bound EPS. The microscopic images of DAPI for aggregates and FITC fluorescence for lectins appeared as blue and green colour, respectively, except in the case of Glycine max, which was TRITC conjugated (orange). Furthermore, both the images of FITC and DAPI were overlaid and prepared using cellSens standard imaging software (Olympus, Tokyo Japan) and Image J software (v. 1.52a). Likewise, the images of TRITC-labelled conjugate and DAPI (orange and blue combination) were processed.

(ii) FT-IR analysis of freshwater and estuarine bacterial pairs and their coaggregates before and after the extraction of CB-EPS

In order to identify the molecules which are probably involved in retaining coaggregation ability in the absence of CB-EPS, the aliquots of the selected estuarine and freshwater biofilm bacterial cell pellets and their coaggregates (formed before and after the extraction of CB-EPS) were lyophilized and subjected to the Fourier- transform infrared spectroscopy (FT-IR) as described above. This analysis has been proven as a powerful tool to understand structural changes occurring in the bacterial cell surfaces in response to environmental changes (Kamnev, 2008). In addition, laboratory experiments were conducted on the bacterial pairs which retained their ability to coaggregate even in the absence of CB-EPS by subjecting them to salinity-stress to assess the impact of salinity-stressed biofilm bacteria on the aggregation process. Briefly, the selected freshwater strains were translocated and grown in ZMB (exposed to high salinity, i.e. 34) and estuarine bacteria in NB (exposed to low salinity, i.e. 5) upto the stationary phase. Furthermore, the coaggregation assays were performed in duplicates as described above, and the aliquots of these coaggregates were lyophilized and desiccated to assess the response of these bacteria to environmental changes using FT-IR.

Results

Experiment I

Biofilm-forming potential using coaggregation assay

Among the total twenty-three strains, ten strains with high biofilm-forming potential were selected based on their strong autoaggregation and coaggregation scores, as depicted in the Electronic Supplementary Material (ESM_2). It was observed that the coaggregation process was growth-phase dependent, i.e., the isolates showed maximum coaggregation during the stationary phase, irrespective of the type of biofilm. The average period of the stationary phase was found to be 48h and 72h for freshwater and estuarine/marine biofilm bacteria, respectively. Out of twenty-three strains, nine isolates (4-freshwater, 5-estuarine) were chosen based on their strong auto-aggregation (i.e. “3” and “4”) and coaggregation scores (i.e. in range of “3” to “4”). Most of the isolates within these freshwater and estuarine, coaggregated with at least one other strain with high coaggregation scores. However, in the case of marine biofilm bacteria, the majority of pairwise combinations demonstrated weak coaggregation scores (i.e. “1”). Except, only one marine biofilm bacteria (M1), which showed the highest auto-aggregation score (i.e. “3”) and coaggregated with most of the strains (ESM_2). Overall, the coaggregation potential based on pairwise combinations was highest in the estuarine biofilm bacteria (62.5%), followed by freshwater (44%) and minimum for marine biofilm bacteria (28%).

Identification of the selected biofilm-forming isolates with high biofilm-forming potential

From the 16S rDNA sequencing data of the selected biofilm-forming bacterial isolates and their comparison with the gene bank database indicated that most of the isolates belonged to *Bacillus* genera followed by *Exiguobacterium* and *Staphylococcus* (accession numbers: MH429953-MH429961, MH620809). Phylogenetic analysis revealed that the *Bacillus* species were clustered together, and several isolates differed in the rDNA sequence compositions (Fig. 2). Most of the biofilm-forming bacteria from estuarine biofilms showed > 99% similarities with *Bacillus* spp. (MH429953.1), *Bacillus indicus* (MH429954.1), *Bacillus cereus* (MH429955.1), and *Staphylococcus lentus* (MH429956.1). Except for one estuarine bacteria, which showed < 98% similarity with *Bacillus cereus* (MH620809.1). On the other hand, freshwater biofilm-forming bacteria showed > 99% similarities with *Exiguobacterium* spp. (MH429958.1 and MH429959.1), *Bacillus subtilis* (MH429960.1) and *Bacillus cereus* (MH429960.1). While, marine biofilm-forming bacteria showed > 99% similarity with *Staphylococcus lentus* (MH429957.1).

Experiment II

Characterization of CB-EPS extracts from selected biofilm-forming isolates with high biofilm-forming potential using FT-IR

The Fourier-transform infrared spectra of cell-bound EPS extracted from the biofilm bacteria is illustrated in Fig. 3. The possible assignments of the absorption bands and their references are tabulated in Table 1a. The spectral patterns of freshwater and marine bacterial EPS differed from the estuarine bacterial EPS (Fig. 3a-c). The pattern was similar for the rest of the freshwater and estuarine biofilm-forming bacteria (ESM_3a-b), except for one of the estuarine bacteria (*Staphylococcus lentus*), which showed a spectral pattern similar to the freshwater bacteria (ESM_3c). The spectra's of the freshwater, estuarine, and marine bacterial CB-EPS displayed a broad peak at around 3600-3200 cm^{-1} indicating the presence of hydroxyl groups, followed by an asymmetrical stretching peak in the range of 1593-1629 cm^{-1} corresponding to ring stretching of mannose or galactose (Fig.3a-c, Table 1a). Moreover, the absorption peaks in the range from 1,000 cm^{-1} to 1,200 cm^{-1} were also noted linked to the presence of C-O-H side groups and C-O-C glycosidic bond vibrations which are characteristics of all sugar derivatives (Fig.3a-c, Table 1a). The presence of carboxylic acids COO⁻ group (strong peak at 1402-1408 cm^{-1}), uronic acids (1111-1112 cm^{-1}), and ester sulphate groups (810-816 cm^{-1}) were also evident in the spectra (Fig. 3a-c, Table 1a). The freshwater and marine bacterial EPS spectrum contained, in addition to spectral bands noted above, the presence of terpenoids and steroids which were evident from peaks at 1475/1473 and 1363/1365 cm^{-1} , respectively (Fig. 3a, 3c, Table 1a). Overall, the spectroscopic results were suggestive of carbohydrate nature of CB-EPS in all the biofilm bacteria, irrespective of types. Therefore, it was further characterized for its sugar content by using HPLC.

Sugar characterization (%) of CB- EPS from biofilm bacteria

The sugar composition (%) of the bacterial cell-bound EPS belonging to different biofilm types is given in Table 2. Furthermore, these sugar compositions were subjected to NMDS to cluster different biofilm bacterial types on the basis of their sugar composition (ESM_4). Nearly all of the freshwater bacterial cell-bound EPS showed the dominance of galactose with a minor contribution of mannose, xylose, and others (Table 2, ESM_4). On the other hand, the estuarine bacterial cell-bound EPS were distinct, wherein mannose was dominant along with galactose, rhamnose, ribose, arabinose and others (Table 2, ESM_4). On the contrary, the marine bacterial cell-bound EPS composition differed, wherein fructose and sorbitol were dominant sugars, along with ribose, and galactose (Table 2, ESM_4). The components of the sugars varied with the biofilm bacterial types; moreover, the

relative proportions of the individual saccharides differed, suggesting that the exopolymer is a heteropolysaccharide (ESM_4). Analysis of Similarity (ANOSIM) also revealed these differences ($R = 0.56$, $p < 0.05$). The results of SIMPER analysis showing overall dissimilarities in the sugar composition and sugars that significantly contributed to differences between biofilm types are tabulated in Table 3. The average dissimilarity was comparable between freshwater and estuarine (43.63%) and freshwater and marine (43.84%), while it was 52.84% between the estuarine and marine group. The mannose, melibiose, galactose, fructose, and D-sorbitol significantly contributed to the dissimilarity between the biofilm types (refer contribution % in Table 3a-c).

Role of CB- EPS in biofilm formation

Most of the biofilm bacteria, including marine, lost their ability to coaggregate in the absence of CB-EPS, which was evident from turbid supernatant after mixing the bacterial suspensions (data not shown). For those bacterial pairs, i.e. *Exiguobacterium* spp., (MH429959) and *Bacillus cereus* (MH429961) from freshwater, and *Bacillus indicus* (MH429954) and *Bacillus cereus* (MH620809) from the estuarine biofilms, which were able to coaggregate, even in the absence of CB-EPS, were chosen for further characterization.

The visualization of the selected freshwater and estuarine biofilm bacterial coaggregates were observed by using epifluorescence microscopy, which showed that two different species were closely associated with one another (Fig. 4a-b). Moreover, this distribution was confirmed by scanning electron microscopy, which revealed the presence of highly dense coaggregates covered by an extracellular EPS, which helped in holding the bacteria together (Fig. 4c-d).

Comparative characterization of freshwater and estuarine bacterial pairs and their coaggregates before (control) and after the extraction of CB-EPS

(i) Characterization of glycoconjugates on coaggregate surfaces using fluorescent markers

The selected coaggregation pairs showed high levels of specific binding to D-mannose and D-glucose residues (alpha polysaccharides as detected by Concanavalin A) as well as N-acetyl-D-glucosamine and sialic acids (as detected by wheat germ agglutinin) (Fig. 5). On the other hand, a very low-level of N-acetyl-D-galactosamine residues (as detected by Glycine max) were associated with coaggregation pairs during the study period. A similar type of expression of these glycoconjugates was observed by these aggregates even after extraction of CB-EPS (Fig. 5).

(ii) FT-IR analysis of freshwater and estuarine bacterial strains and their coaggregates

The infrared spectra of the freshwater and estuarine bacterial strains and coaggregates exhibited marked changes in the spectral regions (as tabulated in Table 1b) before and after the extraction of cell-bound EPS (ESM_5a-b, ESM_6a-b). The FT-IR of freshwater coaggregates showed distinct peaks at 2957, 1658, and 1537 cm^{-1} attributed to $-\text{CH}$ asymmetric stretching of CH_3 in the fatty acids, amide I and II regions of proteins respectively (Table 1b, ESM_5a). On the other hand, a weak peak pattern was observed in the case of the estuarine coaggregated bacteria (ESM_6a-b). One common trend observed in both were notable changes in the peaks 1058-1072 cm^{-1} which were attributed to alterations in the carbohydrate region (Table 1b, ESM_5a, ESM_6a). However, the opposite trend was observed in the expression pattern by these coaggregates after extraction of cell-bound EPS. In the case of estuarine bacteria, the coaggregates showed the involvement of lipids and proteins which was evident from the emergence of peaks at 2956, 1664 (amide I), and at 1535 cm^{-1} (amide II) respectively, as observed in the spectra (Table 1b, ESM_6b). On the other hand, a weak peak pattern was observed in the case of the freshwater coaggregated bacteria (ESM_5b). Except for, the appearance of a peak at 1724 cm^{-1} corresponding to stretching $\text{C}=\text{O}$ of ester functional groups from the membrane lipids and fatty acids (ESM_5b). Moreover, notable alterations were also observed in the carbohydrate spectral region (1200 to 900 cm^{-1}) of both the biofilm bacteria, which could be attributed to compositional alterations in the cell wall or cell membrane (Table 1b, ESM5b, ESM_6b). A similar type of spectral expression pattern was observed by these coaggregates, formed after exposure of these bacterial pairs to salt stress. The spectra observed were indicative of changes that occurred in the surfaces of the individual and coaggregated bacteria when subjected to environmental changes (ESM_5c, ESM_6c). The estuarine biofilm bacteria expressed lipids and proteins which was evident from the emergence of peaks at 2957, 1664 (amide I), and 1535 cm^{-1} (amide II) respectively, different from the freshwater spectra (Table 1b, ESM_5c, ESM_6c). The most remarkable modifications were observed in the carbohydrate spectral region of both the bacterial spectra (1200 to 900 cm^{-1}) due to alterations in the cell membrane along with the appearance of a peak at 1722 cm^{-1} corresponding to the membrane lipids and fatty acids (Table 1b, ESM_5c, ESM_6c).

Discussion

In the present study, the estuarine and freshwater biofilm bacteria showed higher autoaggregation and coaggregation potential as indicated by strong auto- and coaggregation scores, compared to marine biofilm bacteria. This coaggregation potential was growth phase-dependent, i.e., aggregation was observed at the stationary phase. This finding corroborates well with earlier studies which reported growth phase-dependent aggregation in the biofilm bacteria from freshwater and marine

environments (Rickard et al., 2000, 2002; Saravanan et al., 2014). The bacteria possessing the aggregation capabilities, i.e. auto-aggregation and coaggregation, imparts selective advantage over non-coaggregating ones, thereby playing an important role in the development of enhanced biofilm formation via interbacterial interactions (Rickard et al., 2004). On the other hand, weak coaggregation was observed among most of the marine biofilm bacterial strains isolated in this study, except for one marine biofilm-forming bacteria, which showed the highest coaggregation scores. An earlier study by Buswell et al. (1997), reported that low coaggregation scores do not imply weak interactions. Moreover, these coaggregation properties may depend on the relative size or morphologies of bacteria and the density of interacting ligands present on the cell surface (Buswell et al., 1997). Overall, these variations observed in the coaggregation potential among biofilm bacteria within different aquatic environments based on their salinity differences could be attributed to the diverse bacterial species and differences in the mechanisms mediating this process. Besides, the role of pH in influencing this coaggregation process cannot be ruled out for the reason that the pH profiles in the aquatic environments differ, and such changes in physicochemical factors can have a profound effect on the composition and viscosity of the bacterial adhesive exopolymers as well as cell surface molecules, which in turn may influence the coaggregation process. But, this needs further validation.

Although the bacterial strains used in the present study represented only a small proportion of total biofilm bacteria, the coaggregation appeared to be a significant phenomenon within these culturable biofilm-associated bacteria. The 16S rDNA sequencing data of the selected biofilm-forming bacterial isolates and their comparison to the gene bank database indicated that most of the isolates were identified as *Bacillus* genera followed by *Exiguobacterium* and *Staphylococcus*, which are Gram-positive bacteria belonging to Firmicutes. These genera are predominantly found in the oral infections and dental caries as well (Helgason et al., 2000; Raju & Anithal, 2015; Rani et al., 2016; Sakthivel et al., 2016). Moreover, members of Firmicutes have been reported as the most frequent isolates identified from the culturable bacteria diversity in the saline conditions (Kalwasinska et al., 2017; Remonsellez et al., 2018). Phylogenetic analysis revealed that all the *Bacillus* species clustered together differed in the rDNA sequence compositions. Members of genus *Bacillus* are ubiquitous in the terrestrial, freshwater as well as in the seawater habitats (Ruger, 1989). This genus includes several species which can colonize different specialized niches and adapt to changing environmental conditions such as salinity (Khandeparker et al., 2011; Sravankumar et al., 2014). This suggests that *Bacillus* spp. may be one of the many bridging organisms which facilitate the coaggregation with other bacteria, which are incapable of aggregating but needs further

validation. Likewise, in the case of oral biofilms, it is known that the pathogenic bacteria will attach only to biofilms formed by initial colonizers, which are non-pathogenic ones (mostly Gram-positive bacteria) that contribute to coaggregation process and form a suitable favourable environment by producing metabolic end products such as lactate, N-acetyl muramic acid, p-amino benzoic acid etc., for pathogenic ones (mostly Gram-negative bacteria) to adhere (Bowden et al., 1979; Vasudevan, 2017). It is thought-provoking whether such a scenario exists in aquatic biofilm bacteria with *Bacillus* spp., as one of the many other species involved in creating a favourable environment for pathogens to adhere.

As the coaggregation process includes the interaction of different bacteria at the cell surface and involves cell-cell interactions, we focused on characterizing cell-bound EPS and identifying their role in the coaggregation. The nature of cell-bound EPS was characterized more specifically in terms of chemical functional groups using FT-IR. The cell-bound EPS were rich in carbohydrates showing the presence of hydroxyl, carbonyl groups, mannose and uronic acids, which has great relevance in the adhesion, aggregation and cohesion processes (Decho, 1990; Jain & Bhosle, 2008; Casillo et al., 2018). The HPLC analysis revealed the freshwater cell-bound EPS to be a sulphated heteropolysaccharide, wherein galactose was dominant sugar along with terpenoids and steroids as evident from spectra (Fig. 3a, Table 1a, Table 2). These terpenoids are known as the largest class of natural products, which serve as a medium of communication among species, thereby playing a significant role in antagonistic and beneficial interactions among organisms (Gershenson & Dudareva, 2007). Whereas, steroids are mostly chemical signalling compounds which trigger phenotypic changes in microbes via quorum sensing and enhance their adherence to surfaces (Patt et al., 2018). This suggests that these compounds might play an important role in the biofilm formation of these freshwater strains.

On the other hand, the estuarine bacterial EPS, also a sulphated heteropolysaccharide, were dominated by mannose. Although the relative proportions of the other individual sugars differed between the estuarine bacterial strains, it was not significant. This result suggests that diversity in sugar composition could further possibly result in variation in functionality among the estuarine strains. It has been reported that the sugars found in the bacterial EPS facilitate and enhances the bacterial adhesion (van Loosdrecht et al., 1990; Azeredo & Oliveira, 2000; Tsuneda et al., 2003; Cavalcante et al., 2014). The presence of the sulphate moieties in the bacterial EPS provides flexibility to EPS, impart gel-like consistency and thus help in stabilising the polymer, and might also be useful in the aggregation of cells (Bhasker, 2003; Hoagland et al., 1993). Whereas, the cell-bound EPS extract of marine strain showed fructose and sorbitol as dominant sugars along with

terpenoids and steroids. Overall, the sugar composition of estuarine bacterial EPS was more diverse, followed by freshwater and least was observed in the marine. Hence, the sugar composition of the CB-EPS seems to be crucial for strong coaggregation capabilities. However, since the present study included only one marine isolate, it makes the comparison across different aquatic systems rather difficult and requires further validation.

Most of the biofilm bacteria, including marine bacteria used in the present study, lost their ability to coaggregate after extraction of the cell-bound EPS, suggesting the importance of cell-bound EPS in the aggregation process. For those bacterial pairs, i.e. *Exiguobacterium* spp., and *Bacillus cereus* from freshwater, and *Bacillus indicus* and *Bacillus cereus* from the estuarine biofilms, which still retained their ability to coaggregate even after extraction of the cell-bound EPS, were chosen for further studies. The scanning electron micrographs of these coaggregated bacterial pairs revealed that highly dense bacterial aggregates were embedded in an abundant extracellular material. Hence, it was evident that the presence of some specific molecules produced by the coaggregates helped in holding the bacteria together. Earlier studies have investigated the nature of bacterial cell surface molecules using the sugar reversal tests, i.e. by comparing the coaggregation capability in the presence of sugars (Kolenbrander et al., 1993; Rickard, 2000; Kolenbrander et al., 2006; Stevens et al., 2015). Lactose or N-acetyl-D-galactosamine were major sugars reported in blocking coaggregation between bacteria from human oral biofilms (Katharios-Lanwermyer et al., 2014 and references with). However, this does not provide information on the type of the surface molecules associated with the coaggregates. Hence, these coaggregated pairs were characterized for the presence of glycoconjugates using specific fluorescent lectins.

Lectin molecules specifically bind to carbohydrates and thus are powerful tools used for analyzing glycidic structures of microbial origin aggregates (Cavalcante et al., 2014). In the present study, both the estuarine (*Bacillus indicus* and *Bacillus cereus*) and freshwater (*Exiguobacterium* spp., and *Bacillus cereus*) coaggregates showed high levels of specific binding to D-mannose, D-glucose residues and N-acetyl-D-glucosamine/sialic acids and these molecules were expressed even after the extraction of the cell-bound EPS. The mannose is a hexose sugar with more hydroxyl groups than a pentose sugar and is considered as a promotory sugar (Khandeparker & Anil, 2011; Sahoo & Khandeparker, 2018). Both D-glucose and D-mannose serve as important cues for the settlement of *Balanus amphitrite* cyprids (Khandeparker et al., 2002, 2003; Khandeparker & Anil, 2011). The interactions between these sugars and cypris temporary adhesive are most likely to be affected via polar groups. The higher number of hydroxyl groups influence stronger attachment with polar groups of cyprid antennules (Neal & Yule, 1996; Sahoo & Khandeparker, 2018). On the other

hand, sialic acids are sugars, which play an important role in cellular recognition, cell-cell attachment, and signaling (Sigma-Aldrich, 2009). It is well known that several pathogenic bacteria or parasites use surface sialic acids for attachment to the host cell (Sigma-Aldrich, 2009). Moreover, relatively high amounts of these molecules (N-acetyl-D-glucosamine, D-glucose and D-mannose) have been detected in the algal cell wall surfaces as well (Tien et al., 2005). Earlier studies have also reported that N-acetyl-D-glucosamine also plays a significant role in the attachment of fouling diatoms (Bahulikar & Kroth, 2008; Khodse & Bhosle, 2010). A recent study demonstrated the importance of N-acetyl-D-glucosamine expressed by diatoms and its interaction with barnacle shell proteins in facilitating cyprid metamorphosis (Sahoo & Khandeparker, 2018). N-acetyl-D-galactosamine, along with D-glucose and D-mannose produced by haemocytes have been reported as cues for the settlement of *Balanus amphitrite* (Khandeparker et al., 2019). Thus, the results from the present study indicate the involvement of N-acetyl-D-glucosamine/sialic acid, D-mannose, and D-glucose in the bacterial cell-cell interactions, which are similar to the cues reported for the attachment of fouling diatoms and recruitment of larger macrofouling organisms.

FT-IR analysis has been recognized as a powerful tool to understand the structural changes occurring in the bacterial cell surfaces in response to environmental changes (Kamnev, 2008). The biomolecules, mainly sugars, proteins, and lipids in the bacterial membrane have distinct infrared (IR) vibrations that indicate their conformation and physical state (Pan et al., 2017). The results revealed that before the extraction of cell-bound CB-EPS, some peculiar proteins and lipids were expressed by the freshwater coaggregates, as evident from the spectra, probably to carry out cell-cell interactions. On the other hand, after EPS extraction, the proteins and lipids were expressed by the estuarine coaggregates, which possibly helped them in retaining the biofilm-forming capability. Alternatively, the same was not the case with the freshwater bacteria, which coaggregated by expression of lipids in the absence of CB-EPS. An earlier study by Andrews et al. (2010), confirmed the importance of lipids, which can influence and facilitate the attachment of different bacteria. Moreover, in this study, the alterations in the carbohydrate region of the cell membrane were also observed, irrespective of the biofilm types, thus highlighting the importance of carbohydrates in the cell-cell attachment (coaggregation) by biofilm bacterial cells over individual bacterial cells. This result is in accordance with the previous studies by Bengtsson, (1991); Vandervivere & Kirchman, (1993); Cheung et al., (2000).

Formation of biofilms is a quorum-sensing controlled process (involving cell-cell communication and gene regulation); which involves various bacterial physiological activities, including EPS production (Dobretsov et al., 2009; Hmelo, 2017; Jemielita et al., 2018). Moreover,

the secretion of EPS depends on the type of bacteria and environmental factors, which further influences their chemical composition (Sonak, 1998; Khandeparker et al., 2002, 2003; Camilli & Bassler, 2006; Decho & Gutierrez, 2017). As environmental conditions change rapidly, biofilm-forming bacteria possess different mechanisms for sensing and adapting to these changes. One of the important environmental stressors for bacteria is salt stress, i.e. exposure to either high or low salt concentration, which can cause physiological changes in the bacteria and subsequently influence the biofilm formation. Earlier studies have reported that enhanced production of carbohydrates and proteins in the EPS was used as a protective adaptation by bacteria to cope up with salinity stress (Kim & Chong, 2017; Zhao et al., 2016). The present study revealed that the exposure of biofilm-forming bacterial cells (*Bacillus indicus*, *Bacillus cereus* from estuarine and *Exiguobacterium* spp., *Bacillus cereus* from freshwater) to abrupt changes in the salt concentrations (salinity stress) resulted in different physiological response among these bacteria and the subsequent alterations in the surface chemistry of the coaggregates were detected using FT-IR. The estuarine biofilm bacteria could retain their biofilm-forming capability, i.e. by forming aggregates through the expression of proteins and lipids in response to salt-stress. Whereas, the freshwater biofilm bacteria also coped up with the salinity stress and formed aggregates through the expression of lipids. Moreover, this type of expression pattern was also observed by the estuarine and freshwater aggregates in the absence of CB-EPS, and probably this is the mechanism by which these bacteria still retained their biofilm-forming ability under unfavourable conditions. The response and mechanism of *Exiguobacterium* spp., under varying salinities, have been reported earlier, wherein the salt-dependent alterations in the cell membranes were reflected in the concentration of phospholipids that dominated it (Remonsellez et al., 2018). Whereas, the involvement of fatty acids and their composition in the *Bacillus* spp., has been reported in response to a wide variety of adaptations (Diomandé et al., 2015 and references within). Unlike *Bacillus* spp., the exposure of salt-stress had an influence on the intensity of orange colour pigmentation of *Exiguobacterium* strains during the study period (data not shown), indicating some relation between salt-tolerance and pigmentation. One common trend observed in both the biofilm types were notable changes in the carbohydrate region, indicating the significance of carbohydrates in the coaggregation process. Thus, it seems like the salt stress conditions effectively induced quorum sensing in the *Exiguobacterium* spp., and *Bacillus* spp., irrespective of biofilm types, resulting in the alterations in their cell surface chemistry in response to environmental changes, thus retaining their coaggregation potential and these modifications aided in their survival.

Conclusions

The present study is a first report to demonstrate the coaggregation potential of biofilm-forming bacteria from different aquatic environments (freshwater, estuarine, and marine), and identify the molecules involved in their aggregation. The biofilm-forming potential via cell-cell interactions of estuarine and freshwater biofilm bacteria was higher, attributed to cell-bound EPS rich in carbohydrates with distinct sugar composition, compared to marine. The carbohydrate content of the cell-bound EPS was influenced by the environment and varied among the biofilm bacteria. Most of the biofilm bacteria, including marine, lost their ability to coaggregate in the absence of cell-bound EPS suggesting its importance in the aggregation process. The estuarine (*Bacillus indicus* and *Bacillus cereus*) and freshwater (*Exiguobacterium* spp. and *Bacillus cereus*) biofilm bacterial pairs, which retained their ability to coaggregate even in the absence of cell-bound EPS, produced specific biomolecules (D-mannose, D-glucose, N-acetyl-D-glucosamine on the cell surface) in common. However, the underlying mechanism of the formation of estuarine coaggregates differed from freshwater ones, by expression of proteins and lipids. A similar expression pattern was also observed by the estuarine coaggregates after subjecting to salt-stress conditions, and probably this is the mechanism by which estuarine bacteria switch over and still retain their biofilm-forming capability under changing environmental conditions. Thus, it seems that the capability to coaggregate is influenced by the interplay of the environmental factors, biofilm bacterial species and molecules expressed at the cell surface. As biofilms serve as important settlement cues for the recruitment of macrofouling organisms, understanding the role of the molecules expressed by these biofilms via cell-cell interactions and their influence on the larval settlement and recruitment of macrofoulers under different environmental settings is an important topic for future investigation.

Acknowledgements

We are thankful to the Director, National Institute of Oceanography, for his support and encouragement. We are also thankful to Bio-organic chemical laboratory for providing access to FT-IR spectroscopy, and Dr Maria Brenda Mascarenhas for providing access to scanning electronic microscopy (SEM) facility. The first author acknowledges Jawaharlal Nehru Memorial Fund for the award of JNMF Scholarship and is a registered PhD student at the School of Atmospheric, Earth and Ocean Sciences, Goa University. This work was funded by the Ballast Water Management Program, India (Ministry of Shipping and DG shipping) (GAP 2429) and CSIR funded Ocean Finder Program (PSC 0105). This is NIO contribution No #####

References

- Abisado, R.G., Benomar, S., Klaus, J.R., Dandekar, A.A., & J.R. Chandler, 2018. Bacterial quorum sensing and microbial community interactions. *MBio* 9(3): e02331-17
- Adav, S.S., D.J. Lee, & J.Y. Lai, 2008. Intergeneric coaggregation of strains isolated from phenol-degrading aerobic granules. *Applied Microbiology and Biotechnology* 79: 657-661.
- Andrews, J.S., S.A. Rolfe, W.E. Huang, J.D. Scholes, & S.A. Banwart, 2010. Biofilm formation in environmental bacteria is influenced by different macromolecules depending on genus and species. *Environmental Microbiology* 12: 2496-2507.
- Azeredo, J., & R. Oliveira, 2000. The role of exopolymers in the attachment of *Sphingomonas paucimobilis* Biofouling 16: 59-67.
- Bahulikar, R.A. & P.G. Kroth, 2008. The complex extracellular polysaccharides of mainly chain-forming freshwater diatom species from epilithic biofilms. *Journal of Phycology* 44: 1465-1475.
- Basson, A., L.A. Flemming, & H.Y. Chenia, 2008. Evaluation of adherence, hydrophobicity, aggregation, and biofilm development of *Flavobacterium johnsoniae*-like isolates. *Microbial Ecology* 55: 1-14.
- Bengtsson, G. 1991. Bacterial exopolymer and PHB production in fluctuating ground-water habitats. *FEMS Microbiology and Ecology* 86: 15-24
- Bhasker P.V. 2003. Studies on some of aspects of marine microbial polysaccharides. PhD thesis, Goa University
- Bramhachari, P., & S. Dubey, 2006. Isolation and characterization of exopolysaccharide produced by *Vibrio harveyi* strain VB23. *Letters in Applied Microbiology* 43: 571-577.
- Buswell, C.M., Y.M. Herlihy, P.D. Marsh, C.W. Keevil & S.A. Leach, 1997. Coaggregation amongst aquatic biofilm bacteria. *Journal of Applied Microbiology* 83: 477-484.
- Bowden, G.H.W., D.C. Ellwood, & I.R. Hamilton, 1979. Microbial ecology of the oral cavity. In *Advances in Microbial Ecology*. Springer, Boston, MA: 135-217
- Cai, W., L. Xie, Y. Chen, & H. Zhang, 2013. Purification, characterization and anticoagulant activity of the polysaccharides from green tea. *Carbohydrate Polymers* 92: 1086-1090.
- Camilli, A., & B.L Bassler, 2006. Bacterial small-molecule signaling pathways. *Science* 311: 1113–1116.
- Casillo, A., R., Lanzetta, M., Parrilli, & M.M. Corsaro, 2018. Exopolysaccharides from marine and marine extremophilic bacteria: structures, properties, ecological roles and applications. *Marine Drugs* 16(2): 69.
- Cavalcante, T.T.A., N.S.A. Firmino, F.A.S. Tajra, C.R. de Andrade, & R.A. Costa, 2014. Plant lectins as alternative tools against bacterial biofilms. *African Journal of Microbiology Research* 8: 2555-2564.

- Cheung, H.Y., S.Q. Sun, B. Sreedhar, W.M. Ching, & P.A. Tanner, 2000. Alterations in extracellular substances during the biofilm development of *Pseudomonas aeruginosa* on aluminium plates. *Journal of Applied Microbiology* 89: 100-106.
- Cheng, Y.P., Zhang, P., Guo, J.S., Fang, F., Gao, X., & Li, C. (2013). Functional groups characteristics of EPS in biofilm growing on different carriers. *Chemosphere*, 92, 633–638.
- Cheng, Z., X. Meng, H. Wang, M. Chen, & M. Li, 2014. Isolation and characterization of broad spectrum coaggregating bacteria from different water systems for potential use in bioaugmentation. *PloS one*, 9(4): e94220. doi:10.1371/journal.pone.0094220
- Cisar, J.O., P.E. Kolenbrander, & F.C. McIntire, 1979. Specificity of coaggregation reactions between human oral streptococci and strains of *Actinomyces viscosus* or *Actinomyces naeslundii*. *Infection and Immunity* 24: 742-752.
- Clarke, K.R., & R.M. Warwick, 1994. Similarity-based testing for community pattern: the 2-way layout with no replication. *Marine Biology* 118: 167-176.
- Dang, H. & C.R. Lovell, 2016. Microbial surface colonization and biofilm development in marine environments. *Microbiology and Molecular Biology Reviews* 80: 91-138.
- Deepika, G., E. Karunakaran, C.R. Hurley, C.A. Biggs, & D. Charalampopoulos, 2012. Influence of fermentation conditions on the surface properties and adhesion of *Lactobacillus rhamnosus* GG. *Microbial Cell Factories* 11: 116.
- Decho, A.W. 1990. Microbial exopolymer secretions in ocean environments: Their role(s) in food webs and marine processes. *Oceanography and Marine Biology, An Annual Review* 28: 73-153.
- Decho, A.W. & T. Gutierrez, 2017. Microbial extracellular polymeric substances (EPSs) in ocean systems. *Frontiers in Microbiology* 8: 922.
- de Carvalho, C.C.C.R., 2018. Marine biofilms: a successful microbial strategy with economic implications. *Frontiers in Marine Science* 5: 126.
- De Gregoris, T.B., L. Khandeparker, A.C. Anil, E. Mesbahi, J.G. Burgess, & A.S. Clare, 2012. Characterisation of the bacteria associated with barnacle, *Balanus amphitrite*, shell and their role in gregarious settlement of cypris larvae. *Journal of Experimental Marine Biology and Ecology* 413: 7-12.
- Diomandé, S.E., M.H. Guinebretière, V. Broussolle, & J. Brillard, 2015. Role of fatty acids in *Bacillus* environmental adaptation. *Frontiers in Microbiology* 6: 813.
- Dobretsov S, Teplitski M, & V. Paul, 2009. Mini-review: quorum sensing in the marine environment and its relationship to biofouling. *Biofouling* 25: 413–27
- Dobretsov, S. & D. Rittschof, 2020. Love at First Taste: Induction of Larval Settlement by Marine Microbes. *International Journal of Molecular Sciences* 21(3): 731.
- D'souza, F., 2004. Study on bacterial exopolysaccharides and their role in adhesion and corrosion (Doctoral dissertation, Goa University).

- Ellwood, D.C. & D.W. Tempest, 1972. Effects of environment on bacterial wall content and composition. In *Advances in microbial physiology* Academic Press. 7: 83-117.
- Elnahas, M., M. Amin, M. Hussein, V. Shanbhag, A. Ali, & J. Wall, 2017. Isolation, characterization and bioactivities of an extracellular polysaccharide produced from *Streptomyces* sp. MOE6. *Molecules* 22: 1396.
- Fang, F., W.T. Lu, Q. Shan, & J.S. Cao, 2014. Characteristics of extracellular polymeric substances of phototrophic biofilms at different aquatic habitats. *Carbohydrate Polymers* 106: 1-6.
- Freitas, F., V.D. Alves, J. Pais, N. Costa, C. Oliveira, L. Mafra, L. Hilliou, R. Oliveira, & M.A. Reis, 2009. Characterization of an extracellular polysaccharide produced by a *Pseudomonas* strain grown on glycerol. *Bioresources and Technology* 100: 859–865.
- Gibbons R. J. & M. Nygaard, 1970. Inter bacterial aggregation of plaque bacteria. *Archives of Oral Biology* 15: 1397-1400
- Gershenzon, J. & N. Dudareva, 2007. The function of terpene natural products in the natural world. *Nature Chemical Biology* 3: 408.
- Guezennec, J., P. Pignet, Y. Lijour, E. Gentric, J. Ratiskol, & S. Collic-Jouault, 1998. Sulfation and depolymerization of a bacterial exopolysaccharide of hydrothermal origin. *Carbohydrate Polymers* 37: 19-24.
- Guillonneau, R., C. Baraquet, A. Bazire, & M. Molmeret, 2018. Multispecies biofilm development of marine bacteria implies complex relationships through competition and synergy and modification of matrix components. *Frontiers in Microbiology* 9: 1960.
- Hadfield, M.G., 2011. Biofilms and marine invertebrate larvae: what bacteria produce that larvae use to choose settlement sites. *Annual Review of Marine Science* 3: 453-470.
- Hede, N., & L. Khandeparker, 2018. Influence of Darkness and Aging on Marine and Freshwater Biofilm Microbial Communities Using Microcosm Experiments. *Microbial Ecology* 76: 314-317.
- Helgason, E., D.A. Caugant, I. Olsen & A.B. Kolsto. 2000. Genetic structure of population of *Bacillus cereus* and *B. thuringiensis* isolates associated with periodontitis and other human infections. *Journal of Clinical Microbiology* 38: 1615–1622
- Hmelo, L.R., 2017. Quorum sensing in marine microbial environments. *Annual Review of Marine Science* 9: 257-281.
- Hoagland, K.D., J.R. Rosowski, M.R. Gretz, & S.C. Roemer, 1993. Diatom extracellular polymeric substances: Function, fine structure, chemistry, and physiology. *Journal of Phycology* 29: 537-566.
- Irie, Y., & M.R. Parsek, 2008. Quorum sensing and microbial biofilms. In *Bacterial biofilms* Springer, Berlin, Heidelberg. pp. 67-84.
- Jain, A., & N.B. Bhosle, 2008. Role of β 1-4 linked polymers in the biofilm structure of marine *Pseudomonas* sp. CE-2 on 304 stainless steel coupons. *Biofouling* 24:283-291.
- Jain, A., & N.B. Bhosle, 2009. Biochemical composition of the marine conditioning film: implications for bacterial adhesion. *Biofouling* 25: 13-19.

- Jemielita, M., Wingreen, N.S. & B.L. Bassler, 2018. Quorum sensing controls *Vibrio cholerae* multicellular aggregate formation. *Elife*, 7: p.e42057.
- Katharios-Lanwermeier, S., C. Xi, N.S. Jakubovics, & A.H. Rickard, 2014. Mini-review: microbial coaggregation: ubiquity and implications for biofilm development. *Biofouling* 30: 1235-1251.
- Kalwasinska, A., T. Felföldi, A. Szabó, E. Deja-Sikora, P. Kosobucki, & M. Walczak, 2017. Microbial communities associated with the anthropogenic, highly alkaline environment of a saline soda lime, Poland. *Antonie Van Leeuwenhoek* 110: 945–962.
- Kamnev, A.A., 2008. FT-IR spectroscopic studies of bacterial cellular responses to environmental factors, plant-bacterial interactions and signalling. *Journal of Spectroscopy*, 22: 83-95.
- Kavita, K., A. Mishra, & B. Jha, 2011. Isolation and physico-chemical characterisation of extracellular polymeric substances produced by the marine bacterium *Vibrio parahaemolyticus*. *Biofouling* 27, 309–317.
- Kavita, K., A. Mishra, & B. Jha, 2013. Extracellular polymeric substances from two biofilm forming *Vibrio* species: Characterization and applications. *Carbohydrate Polymers* 94, 882–888.
- Kavita, K., V.K. Singh, A. Mishra, & B. Jha, 2014. Characterisation and anti-biofilm activity of extracellular polymeric substances from *Oceanobacillus iheyensis*. *Carbohydrate Polymers* 101: 29-35.
- Kerr, C.J., K.S. Osborn, A.H. Rickard, G.D. Robson, & P.S. Handley, 2003. Biofilms in water distribution systems. In M. Duncan and N.J. Horan (ed.), *Water and wastewater engineering*. Academic Press, London, United Kingdom. 757-776.
- Kolenbrander, P.E., N. Ganeshkumar, F.J. Cassels, & C.V. Hughes, 1993. Coaggregation: specific adherence among human oral plaque bacteria. *The FASEB Journal* 7: 406-413.
- Kolenbrander, P.E., Jr, R.J. Palmer A.H. Rickard, N.S. Jakubovics, N.I. Chalmers, & P.I Diaz, 2006. Bacterial interactions and successions during plaque development. *Periodontology* 42: 47-79.
- Khandeparker, L., A.C. Anil, & S. Raghukumar, 2002. Factors regulating the production of different inducers in *Pseudomonas aeruginosa* with reference to larval metamorphosis in *Balanus amphitrite*. *Aquatic Microbial Ecology* 28: 37-54.
- Khandeparker, L., A. C. Anil & S. Raghukumar, 2003. Barnacle larval destination: piloting possibilities by bacteria and lectin interaction. *Journal of Experimental Marine Biology and Ecology* 289: 1–13.
- Khandeparker, L. & A.C. Anil, 2011. Role of conspecific cues and sugars in the settlement of cyprids of the barnacle, *Balanus amphitrite*. *Journal of Zoology* 284(3): 206-214.
- Khandeparker, R., P. Verma, R.M. Meena, & D.D. Deobagkar, 2011. Phylogenetic diversity of carbohydrate degrading culturable bacteria from Mandovi and Zuari estuaries, Goa, west coast of India. *Estuarine, Coastal and Shelf Science* 95: 359-366.
- Khandeparker, L., N. Hede, R. Eswaran, A. Usgaonkar & A.C. Anil, 2017. Microbial dynamics in a tropical monsoon influenced estuary: Elucidation through field observations and microcosm experiments on biofilms. *Journal of Experimental Marine Biology and Ecology* 497: 86-98.

- Khandeparker, L., A.C. Anil, & D.V. Desai, 2019. Immuno-modulation of settlement cues in the barnacle, *Amphibalanus amphitrite*: significance of circulating haemocytes. *Hydrobiologia* 830: 229-241.
- Khodse, V.B. & N.B. Bhosle, 2010. Differences in carbohydrate profiles in batch culture grown planktonic and biofilm cells of *Amphora rostrata* Wm. Sm. *Biofouling* 26: 527-537.
- Kim, L.H. & T.H. Chong, 2017. Physiological responses of salinity-stressed *Vibrio* sp. and the effect on the biofilm formation on a nanofiltration membrane. *Environmental science & technology* 51(3): 1249-1258.
- Kodali, V.P., S. Das, & R.K. Sen, 2009. An exopolysaccharide from a probiotic: biosynthesis dynamics, composition and emulsifying activity. *Food Research International* 42: 695–699.
- Kragh, K.N., J.B. Hutchison, G. Melaugh, C. Rodesney, A.E. Roberts, Y. Irie, P.Ø. Jensen, S.P. Diggle, R.J. Allen, V. Gordon, & T. Bjarnsholt, 2016. Role of multicellular aggregates in biofilm formation. *MBio* 7: pp.e00237-16.
- Kumar, K.V., Pal, A., Bai, P., Kour, A., Sheeba, E., Rajarajan, P., Kausar, A., Chatterjee, M., Prasad, G., Balayan, S. & P. Dutta, 2019. Co-aggregation of bacterial flora isolated from the human skin surface. *Microbial Pathogenesis* 135: p.103630.
- Kviatkovski, I. & D. Minz, 2015. A member of the Rhodobacteraceae promotes initial biofilm formation via the secretion of extracellular factor (s). *Aquatic Microbial Ecology* 75(2): 155-167.
- Lorite, G.S., C.M. Rodrigues, A.A. De Souza, C. Kranz, B. Mizaikoff, & M.A. Cotta, 2011. The role of conditioning film formation and surface chemical changes on *Xylella fastidiosa* adhesion and biofilm evolution. *Journal of colloid and interface science* 359: 289-295.
- Ledder, R.G., T. Madhwani, P.K. Sreenivasan, W. De Vizio, & A.I. McBain, 2009. An in vitro evaluation of hydrolytic enzymes as dental plaque control agents. *Journal of Medical Microbiology* 58: 482-491.
- Lloyd, A.G., K.S. Dodgson, R.G. Price, & F.A. Rose, 1961. I. Polysaccharide sulphates. *Biochimica et Biophysica Acta* 46: 108-115.
- Malik, A., M., Sakamoto, S. Hanazaki, M. Osawa, T. Suzuki, M. Tochigi, & K. Kakii, 2003. Coaggregation among non-flocculating bacteria isolated from activated sludge. *Applied and Environmental Microbiology* 69: 6056-6060
- Melaugh, G., J. Hutchison, K.N. Kragh, Y. Irie, A.E.L. Roberts, T. Bjarnsholt, S.P. Diggle, V.D. Gordon, & R.J. Allen, 2015. Shaping the growth behaviour of bacterial aggregates in biofilms. *arXiv:1506.08168*
- Min, K.R. & A.H. Rickard, 2009. Coaggregation by the freshwater bacterium *Sphingomonas natatoria* alters dual-species bio- film formation. *Applied and Environmental Microbiology* 75: 3987–3997.
- Min, K.R., Zimmer, M.N. & A.H. Rickard, 2010. Physicochemical parameters influencing coaggregation between the freshwater bacteria *Sphingomonas natatoria* 2.1 and *Micrococcus luteus* 2.13. *Biofouling* 26(8): 931-940.

- Mora-Gómez, J.A. Freixa, N. Perujo, & L. Barral-Fraga, 2016. Limits of the biofilm concept and types of aquatic biofilms. *Aquatic Biofilms: Ecology, Water Quality and Wastewater Treatment*. 3-27
- Naumann, D., 2000. Infrared spectroscopy in microbiology. *Encyclopedia of Analytical Chemistry* 102: p.131.
- Neal, A. L. & A. B. Yule, 1996. The effects of dissolved sugars upon the temporary adhesion of barnacle cyprids. *Journal of the Marine Biological Association of the United Kingdom* 76: 649-655.
- Ojeda, J.J., M.E. Romero-González, & S.A. Banwart, 2009. Analysis of bacteria on steel surfaces using reflectance micro-Fourier transform infrared spectroscopy. *Analytical Chemistry* 81: 6467-6473.
- Pan, M., K.K. Kumaree, & N.P. Shah, 2017. Physiological changes of surface membrane in *Lactobacillus* with prebiotics. *Journal of Food Science*, 82: 744-750.
- Patt, M.W., L. Conte, M. Blaha, & B.J. Plotkin, 2018. Steroid hormones as interkingdom signaling molecules: Innate immune function and microbial colonization modulation. *Aims Molecular Science* 5: 117-130.
- Palmer Jr, R.J., S.M. Gordon, J.O. Cisar, & P.E. Kolenbrander, 2003. Coaggregation-mediated interactions of *Streptococci* and *Actinomyces* detected in initial human dental plaque. *Journal of Bacteriology* 185: 3400-3409.
- Purevdorj-Gage, B., W.J. Costerton, & P. Stoodley, 2005. Phenotypic differentiation and seeding dispersal in non-mucoid and mucoid *Pseudomonas aeruginosa* biofilms. *Microbiology* 151: 1569-1576.
- Rani, A.A., S. Jeeva, S.M.J. Punitha, N.P. Lexshmi, & J.R. Brindha, 2016. Biochemical and molecular analysis of bacteria isolated from dental caries. *Journal of Chemical and Pharmaceutical Research* 8: 512-519.
- Raju K.S., & L. Anitha, 2015. Isolation and Identification of Oral flora from individuals belonging to ages 7 to 16 years. *Research Journal of Science and IT Management* 4: 5-11.
- Rickard, A.H., S.A. Leach, C.M. Buswell, N.J. High, & P.S. Handley, 2000. Coaggregation between aquatic bacteria is mediated by specific-growth-phase-dependent lectin-saccharide interactions. *Applied Environmental Microbiology* 66: 431-434.
- Rickard, A.H., S.A. Leach, L.S. Hall, C.M. Buswell, N.J. High, & P.S. Handley, 2002. Phylogenetic relationships and coaggregation ability of freshwater biofilm bacteria. *Applied Environmental Microbiology* 68: 3644-3650.
- Rickard, A.H., P. Gilbert, N.J. High, P.E. Kolenbrander, & P.S. Handley, 2003. Bacterial coaggregation: an integral process in the development of multi-species biofilms. *Trends in Microbiology* 11: 94-100.
- Rickard, A.H., P. Gilbert, & P.S. Handley, 2004 Influence of growth environment on coaggregation between freshwater biofilm bacteria *Journal of Applied Microbiology* 96: 136773.

- Remonsellez, F., J. Castro-Severyn, P.M. Aguilar Espinosa, J. Fortt, C. Salinas, S. Barahona, J. León, C. Pardo-Esté, B. Fuentes, C. Areche, & K. Hernández, 2018. Characterization and salt response in recurrent halotolerant *Exiguobacterium* spp. SH31 isolated from sediments of Salar de Huasco, Chilean Altiplano. *Frontiers in Microbiology* 9: 2228.
- Ruger, H.J., 1989. Benthic studies of the northwest African upwelling region psychrophilic bacterial communities from areas with different upwelling intensities. *Marine Ecological Progress Series* 57: 45-52.
- Rumbaugh K.P., & A. Armstrong, 2014. The Role of Quorum Sensing in Biofilm Development. In: Rumbaugh K., Ahmad I. (eds) *Antibiofilm Agents*. Springer Series on Biofilms, vol 8. Springer, Berlin, Heidelberg 97-113
- Sahoo, G. & L. Khandeparker, 2018. Role of epibiotic diatoms isolated from the barnacle shell in the cyprid metamorphosis of *Balanus amphitrite*. *Hydrobiologia* 822: 129-142.
- Sakthivel, M., P.M. Ayyasamy, & D. Arvind Prasanth, 2016. Identification and antimicrobial susceptibility testing of pathogenic microorganism from dental patients *Asian Journal of Pharmaceutical and Clinical Research* 9: 226-230.
- Saravanan, N., P. Verma, V.P. Mol, R.S. Kumar, S.T. Somasundaram, G. Dharani, & R. Kirubakaran, 2014. Role of microbial aggregation in biofilm formation by bacterial strains isolated from offshore finfish culture environment. *Indian Journal of Geo-Marine Sciences* 43: 2118-2129.
- Sauer, K., A.K. Camper, G.D. Ehrlich, J.W. Costerton, & D.G. Davies 2002. *Pseudomonas aeruginosa* displays multiple phenotypes during development as a biofilm. *Journal of Bacteriology* 184: 1140-1154
- Seedevi, P., S. Sudharsan, S.V. Kumar, A. Srinivasan, S. Vairamani, & A. Shanmugan, 2013. Isolation and characterization of sulphated polysaccharides from *Codium tomentosum* (J. Stackhouse, 1797) collected from southeast coast of India. *Advances in Applied Science Research* 4: 72-77.
- Sheng, G.P., H.Q. Yu, & Z. Yu, 2005. Extraction of extracellular polymeric substances from the photosynthetic bacterium *Rhodospseudomonas acidophila*. *Applied Microbiology and Biotechnology* 67: 125-130.
- Simões, L.C., M. Simoes, & M.J. Vieira, 2008. Intergeneric coaggregation among drinking water bacteria: evidence of a role for *Acinetobacter calcoaceticus* as a bridging bacterium. *Applied and Environmental Microbiology* 74: 1259-1263.
- Sigma-Aldrich, 2009. *Glycobiology*. Life Science BioFiles 5: 1-32
- Smyth, K. & M. Elliott, 2016. Effects of changing salinity on the ecology of the marine environment. In: Solan M, Whiteley NM (eds) *Stressors in the marine environment*. Oxford University Press, Oxford, pp 161–174.
- Sonak, S.M., 1998. *Studies on marine fouling bacteria* (Doctoral dissertation, Goa University).
- Sravankumar, G., Y.V.K. Durgaprasad, T. Ramana, & C.S.L.V. Devi, 2014. Isolation and identification of bacteria from marine biofilm on the artificial plat forms (iron panels) from Visakhapatnam coast, India. *Indian Journal of Geo-Marine Sciences* 43: 961-965

- Stewart, P.S., & J.W. Costerton, 2001. Antibiotic resistance of bacteria in biofilms. *The Lancet*. 358: 135-138
- Strathmann, M., J. Wingender, & H.C. Flemming, 2002. Application of fluorescently labelled lectins for the visualization and biochemical characterization of polysaccharides in biofilms of *Pseudomonas aeruginosa*. *Journal of Microbiological Methods* 50: 237-248.
- Stratil, S.B., Neulinger, S.C., Knecht, H., Friedrichs, A.K. & M. Wahl, 2014. Salinity affects compositional traits of epibacterial communities on the brown macroalga *Fucus vesiculosus*. *FEMS Microbiology Ecology* 88(2): 272-279.
- Stevens, M.R., T.L. Luo, J. Vornhagen, N.S. Jakubovics, J.R. Gilsdorf, C.F. Marrs, T. Møretrø, & A.H. Rickard, 2015. Coaggregation occurs between microorganisms isolated from different environments. *FEMS Microbiology Ecology* 91: p.fiv123.
- Stoodley, P., L. Hall-Stoodley & H.M. Lappin-Scott, 2001. Detachment, surface migration, and other dynamic behavior in bacterial biofilms revealed by digital time-lapse imaging. *Methods Enzymology* 337: 306-319.
- Suh, H.H., G.S. Kwon, C.H. Lee, H.S. Kim, H.M. Oh, & B.D. Yoon, 1997. Characterization of bioflocculant produced by *Bacillus* sp. DP-152. *Journal of Fermentation and Bioengineering* 84: 108-112.
- Tallon, R., P. Bressollier, & M.C. Urdaci, 2003. Isolation and characterization of two exopolysaccharides produced by *Lactobacillus plantarum* EP56. *Research in Microbiology* 154: 705-712.
- Tamura, K., G. Stecher, D. Peterson, A. Filipski, & S. Kumar, 2013. MEGA6: molecular evolutionary genetics analysis version 6.0 *Molecular Biology and Evolution* 30: 2725-2729.
- Tien, C.J., D.C. Sigee, & K.N. White, 2005. Characterization of surface sugars on algal cells with fluorescein isothiocyanate-conjugated lectins. *Protoplasma*, 225: 225-233.
- Trunk, T., Khalil, H. S., & J.C. Leo, 2018. Bacterial autoaggregation. *AIMS microbiology* 4: 140.
- Tsuneda, S., H. Aikawa, H. Hayashi, A. Yuasa, & A. Hirata, 2003. Extracellular polymeric substances responsible for bacterial adhesion onto solid surface. *FEMS Microbiology Letters* 223: 287-292.
- Qian, P.Y., Lau, S.C., Dahms, H.U., Dobretsov, S. & T. Harder, 2007. Marine biofilms as mediators of colonization by marine macroorganisms: implications for antifouling and aquaculture. *Marine Biotechnology* 9(4): 399-410.
- van Loosdrecht, M., W. Norde, Lyklema, L. & J. Zehnder, 1990. Hydrophobic and electrostatic parameters in bacterial adhesion. *Aquatic Sciences* 51: 103-114.
- Vandervivere, P. & D.L. Kirchman, 1993. Attachment stimulates exopolysaccharide synthesis by a bacterium. *Applied and Environmental Microbiology* 59: 3280-3286.
- Vasudevan, R. 2017. Dental Plaques: Microbial Community of the Oral Cavity. *Journal of Microbiology and Experimentation* 4: 1-9.

Vornhagen, J., M. Stevens, D.W. McCormick, S.E. Dowd, J.N. Eisenberg, B.R. Boles, & A.H. Rickard, 2013. Coaggregation occurs amongst bacteria within and between biofilms in domestic showerheads. *Biofouling* 29: 53-68.

Wahl, M., Goecke, F., Labes, A., Dobretsov, S. & F. Weinberger, 2012. The second skin: ecological role of epibiotic biofilms on marine organisms. *Frontiers in Microbiology* 3: 292.

Watnick, P. & R. Kolter, 2000. Biofilm, city of microbes. *Journal of Bacteriology* 182: 2675-2679.

Zeng, J., J.M. Gao, Y.P. Chen, P. Yan, Y. Dong, Y. Shen, J.S. Guo, N. Zeng, & P. Zhang, 2016. Composition and aggregation of extracellular polymeric substances (EPS) in hypersaline and municipal wastewater treatment plants. *Scientific Reports* 6: 26721.

Zhao, M., N. Yang, B. Yang, Y. Jiang, & G. Zhang, 2007. Structural characterization of water-soluble polysaccharides from *Opuntia monacantha* cladodes in relation to their anti-glycated activities. *Food Chemistry* 105: 1480-1486.

Zhao, L., She, Z., Jin, C., Yang, S., Guo, L., Zhao, Y. & M. Gao, 2016. Characteristics of extracellular polymeric substances from sludge and biofilm in a simultaneous nitrification and denitrification system under high salinity stress. *Bioprocess and Biosystems Engineering* 39(9): 1375-1389.

Legend to Tables

Table 1 a) Interpretation of infrared (IR) spectra and peak assignments of the cell-bound EPS and b) Interpretation of IR spectra of the bacterial cell pellets. Refer to the electronic supplementary material (ESM_5 and ESM_6), for the Fourier-transformed infrared (FT-IR) spectra's of the freshwater and estuarine bacterial cell pellets and coaggregates.

Table 2 Composition (%) of sugars in the cell-bound EPS extracted from biofilm bacteria with high biofilm-forming potential from different aquatic environments. F = Freshwater, E = Estuarine, M = Marine, spp. = species, Rha = Rhamnose, Rib = Ribose, Xyl = Xylose, Arab = Arabinose, GlcNAc = N-acetyl-D-glucosamine, Fruc = Fructose, Man = Mannose, Gal = Galactose.

Table 3 SIMPER analysis showing sugars that contributed to the differences among the biofilm types. a) Freshwater and Estuarine, b) Freshwater and Marine, and c) Estuarine and Marine. Av. Diss = Average dissimilarity, Contrib % = Contribution, Cum. % = Cumulative %, Av. Abund = Average abundance.

Legends to figures

Fig. 1 The schematic illustration of the experimental design. ZMB = Zobell Marine broth, NB = Nutrient broth, EPS = Extracellular polymeric substances, FT-IR = Fourier-transform infrared spectroscopy, SEM = Scanning Electron microscopy, HPLC = High-pressure liquid chromatography.

Fig. 2 Phylogenetic relationship of the chosen biofilm isolates from the freshwater, estuarine, and marine biofilms based on 16S rRNA gene sequence analysis. The sequences obtained from the present study are highlighted in blue for freshwater, pink for estuarine and orange colour for marine. Scale bar, 0.01 substitutions per nucleotide position. sp. = species

Fig. 3 Fourier-transform infrared (FT-IR) spectra's of cell-bound bacterial EPS from representative (a) freshwater, (b) estuarine, and (c) marine biofilm-forming bacteria. The freshwater bacterial EPS spectra are represented in green colour, estuarine bacterial EPS spectra in orange colour, and marine bacterial EPS spectra in pink colour. The zoomed infrared (1800 - 600 cm^{-1}) spectral section is shown in black colour. The spectral pattern for the other freshwater and estuarine biofilm-forming bacteria was similar, except for one of the estuarine (MH429956.1), which showed a spectral pattern similar to the freshwater bacteria.

Fig. 4 Visualization of coaggregates using epifluorescence microscopy (1000x magnification) from (a) freshwater, and (b) estuarine biofilm bacterial pairs (cultures grown till stationary phase), stained either with DAPI (blue) or SYBR green nucleic acid (green) nucleic acid stain, and scanning electron microscopy (SEM) images of coaggregates (2500x and 6000x magnification) formed by (c) freshwater, and (d) estuarine biofilm bacterial pairs (cultures grown till stationary phase).

Fig. 5 Fluorescent labelling of glycoconjugates associated with coaggregates using epifluorescence microscopy (1000x magnification). Con A: Concanavalin A, WGA: Wheat germ agglutinin, and Glycine Max (Soya bean agglutinin SBA). Bacterial coaggregation pairs are visible as blue while D-mannose/ D-glucose residues (as detected by Con A) and N-acetyl-D-glucosamine and sialic acids (as detected by WGA) are visible as green. In the case of Glycine Max, bacterial coaggregation pairs are visible as blue and N-acetyl-D-galactosamine as orange.

Legends to Electronic Supplementary Material

ESM_1 (a) Chromatograms of 19 sugar standards, and (b) Sugars standards with their retention times

ESM_2 Visual aggregation scores exhibited by biofilm bacteria at stationary phase during auto- and coaggregation assay carried out in pairwise combinations between the (a) freshwater, (b) estuarine, and (c) marine biofilm bacterial isolates. Values are noted after 24 hours of incubation. E = Estuarine, F = Freshwater, M = Marine.

ESM_3a Fourier-transform infrared (FT-IR) spectra's of cell-bound EPS extracted from freshwater biofilm-forming bacteria. The freshwater bacterial EPS spectra is represented in green colour. The zoomed infrared ($1800 - 600 \text{ cm}^{-1}$) spectral section is shown in black colour. F= Freshwater.

ESM_3b Fourier-transform infrared (FT-IR) spectra's of cell-bound EPS extracted from estuarine biofilm-forming bacteria. The estuarine bacterial EPS spectra in orange colour. The zoomed infrared ($1800 - 600 \text{ cm}^{-1}$) spectral section is shown in black colour. E = Estuarine.

ESM_3c Fourier-transform infrared (FT-IR) spectra's of cell-bound EPS extracted from estuarine biofilm-forming bacteria depicting spectral pattern similar to the freshwater bacteria. The estuarine bacterial EPS spectra in orange colour. The zoomed infra-red ($1800 - 600 \text{ cm}^{-1}$) spectral section is shown in black colour. E = Estuarine.

ESM_4 Non-metric multidimensional scaling (NMDS) analysis of sugars in the cell-bound EPS extracted from biofilm-forming bacteria. F = freshwater (green up triangle), E = estuarine (dark blue down triangle), M = marine (blue square). The circle represents the length of a vector with a perfect correlation ($R = 1$).

ESM_5 Fourier-transform infrared (FT-IR) spectra's of bacterial cell pellets and coaggregated freshwater biofilm bacteria (a) before extraction of cell-bound EPS, (b) after extraction of cell-bound EPS, and (c) response to salt-stress. Encircles (black) indicate notable changes in the spectral patterns between cell pellets and freshwater coaggregates.

ESM_6 Fourier-transform infrared (FT-IR) spectra's of bacterial cell pellets and coaggregated estuarine bacteria (a) before extraction of cell-bound EPS, (b) after extraction of cell-bound EPS, and (c) response to salt stress. Encircles (black) indicate notable changes in the spectral patterns between cell pellets and estuarine coaggregates.

Table 1

a) Interpretation of infrared (IR) spectra and peak assignments of the cell-bound EPS

Wave number (cm ⁻¹)	Molecular vibrations of functional groups and biomolecule contributor	References
3600-3200 cm ⁻¹	Broad O–H stretching absorption peak indicating the presence of hydroxyl groups, which are characteristics for carbohydrates	Khandeparker et al., 2002; Seedeve et al., 2013; Zeng et al., 2016; Elnahas et al., 2017
3000-2800 cm ⁻¹	C-H stretching vibration band of the aliphatic CH ₂ group by fatty acids and lipids	Cheng et al., 2013; Fang et al., 2014
1593-1629 cm ⁻¹	presence of an asymmetrical stretching peak corresponding to ring stretching of mannose or galactose	Freitas et al., 2009; Kavita et al., 2011; 2013, 2014
Peaks at 1527 & 1533 cm ⁻¹	C-N stretching vibrations in combination with N-H bending of proteins (Amide I and Amide II bands)	Lorite et al., 2011; Fang et al., 2014
1402-1408 cm ⁻¹	symmetric stretching of the carboxylic acids COO ⁻ group	Zhao et al., 2007; Lorite et al., 2011
Peaks at 1475 & 1363 cm ⁻¹	presence of terpenoids and steroids	Khandeparker et al., 2002
1,000 -1125 cm ⁻¹	O-acetyl ester linkage bonds indicating the presence of uronic acids	Bramhachari & Dubey, 2006; Kavita et al., 2014
1,000-1,200 cm ⁻¹	C-O-H side groups and C-O-C glycosidic bond vibrations which are characteristics of all sugar derivatives	Suh et al., 1997; Sheng et al., 2005; Bramhachari & Dubey, 2006; Cai et al., 2013; Kavita et al., 2013
Peaks at 810-816 cm ⁻¹	Presence of ester sulphate groups	Lloyd et al., 1961; D'souza, 2004; Seedeve et al. 2013; Guezennec et al., 1998
858-862 cm ⁻¹	Presence of α-glycosidic linkages between individual glycosyl residues	Kodali et al., 2009

Table 1

b) Interpretation of infrared (IR) spectra and peak assignments of the cell-bound EPS

<u>Wave number (cm⁻¹)</u>	<u>Molecular vibrations of functional groups and biomolecule contributor</u>	<u>References</u>
<u>3000 – 2800 cm⁻¹</u>	<u>Membrane lipids and fatty acids</u>	Naumann, 2000 *Ojeda et al., 2009 *Deepika et al., 2012
<u>*1739 – 1725 cm⁻¹</u>	<u>stretching C=O of ester functional groups from the membrane lipids and fatty acids</u>	
<u>1700 – 1500 cm⁻¹</u>	<u>Proteins and peptides containing Amide I and II bonds</u>	
<u>1500 – 1200 cm⁻¹</u>	<u>Mixed region which includes</u> (1) <u>Fatty acids around 1468, 1455</u> (2) <u>P=O stretching of PO₄- (phosphodiester, backbone of nucleic acids) around 1250-1200</u> (3) <u>Amide III band of proteins around 1350-1240</u>	
<u>1200 – 900 cm⁻¹</u>	<u>Carbohydrate region</u>	
<u>900 – 600 cm⁻¹</u>	<u>Fingerprint region</u>	

Refer to the electronic supplementary material (ESM_5 and ESM_6) for the Fourier-transformed infrared (FT-IR) spectra's of the freshwater and estuarine bacterial cell pellets and coaggregates.

Table 2 Composition (%) of sugars in the cell bound EPS extracted from biofilm bacteria from different aquatic environments.

	Rha	Rib	Xyl	Arab	GlcNAc	Fruc	Man	Glu	Sorbitol	Mannitol	Gal	Sucrose	Inositol	Cellobiose	Maltose	Lactose	Melibiose	Trehalose
Freshwater																		
F1 (<i>Exiguobacterium</i> spp.)	0.00	3.7 3	10.23	3.22	0.00	0.00	22.40	0.00	12.04	0.00	18.02	1.80	2.40	2.20	7.00	3.92	9.10	3.94
F2 (<i>Exiguobacterium</i> spp.)	0.00	2.7 0	6.90	0.00	0.00	0.00	24.50	0.00	3.10	0.60	47.00	1.60	0.40	1.70	3.70	2.30	3.30	2.20
F3 (<i>Bacillus subtilis</i>)	0.00	6.0 4	9.82	2.97	0.00	4.23	14.17	0.00	7.36	0.00	24.37	0.44	3.20	2.60	4.50	4.00	9.03	7.27
F4 (<i>Bacillus cereus</i>)	0.16	0.8 9	5.75	7.36	0.00	12.11	14.37	0.00	8.06	1.70	20.46	2.88	1.73	4.65	7.00	4.27	5.36	3.25
Estuarine																		
E1 (<i>Bacillus</i> spp.)	0.00	0.7 2	0.00	0.35	0.07	0.00	61.43	0.00	4.49	0.37	5.36	1.15	2.17	3.14	3.88	5.95	7.92	3.00
E2 (<i>Bacillus cereus</i>)	3.29	4.7 0	0.00	0.00	0.00	0.00	0.00	0.61	5.39	0.00	19.58	3.29	3.28	4.08	5.88	8.02	37.65	4.23
E3 (<i>Bacillus indicus</i>)	1.76	5.4 5	4.11	6.13	0.00	2.79	19.08	0.00	4.42	0.85	12.90	1.54	2.63	3.29	4.37	6.87	20.09	3.72
E4 (<i>Bacillus cereus</i>)	0.00	2.3 9	5.88	2.95	1.38	0.00	59.37	0.00	0.00	0.34	6.05	1.61	1.23	1.47	1.99	3.95	9.00	2.39
E5 (<i>Staphylococcus</i> <i>lentus</i>)	0.00	10. 50	0.00	7.60	1.00	5.70	0.00	0.00	0.00	0.40	14.60	2.50	6.30	5.60	8.50	11.30	21.50	4.50
Marine																		
M1 (<i>Staphylococcus</i> <i>lentus</i>)	0.00	10. 32	0.00	0.00	0.00	19.76	0.00	0.00	22.54	1.75	20.61	1.36	1.25	2.63	4.59	5.30	7.65	2.24

F = Freshwater, E = Estuarine, M = Marine, spp. = species, Rha = Rhamnose, Rib = Ribose, Xyl = Xylose, Arab = Arabinose, GlcNAc = N-acetyl-D-glucosamine, Fruc = Fructose, Man = Mannose, Gal = Galactose.

Table 3: SIMPER analysis showing sugars that contributed to the differences among the biofilm types. a) Freshwater and Estuarine, b) Freshwater and Marine, and c) Estuarine and Marine.

Av. Diss = average dissimilarity, Contrib% = Contribution, Cum. % = Cumulative %, Av. Abund = average abundance.

a) Average dissimilarity = 43.63						
Group	Freshwater			Estuarine		
Sugars	Av. Diss	Contrib%	Cum.%	Av. Abund	Av. Abund	Diss/SD
Mannose	11.15	25.55	25.55	18.88	27.98	1.79
Melibiose	7.65	17.53	43.09	6.7	22.84	1.71
Galactose	6.25	14.32	57.4	27.48	14.16	1.1
Xylose	3.25	7.45	64.85	8.15	3.72	2.56
Lactose	2.54	5.83	70.68	3.63	9.12	3.02
D-Sorbitol	2.3	5.28	75.96	7.65	3.42	1.47
Fructose	1.97	4.53	80.49	4.08	1.7	1.01
Arabinose	1.68	3.84	84.33	3.4	4.32	1.43
Ribose	1.57	3.59	87.92	3.33	5.56	1.22
Inositol	0.91	2.09	90.01	1.93	3.76	1.13
b) Average dissimilarity = 43.84						
Group	Freshwater			Marine		
Sugars	Av. Diss	Contrib%	Cum.%	Av. Abund	Av. Abund	Diss/SD
Mannose	9.44	21.54	21.54	18.88	0	9.44
Fructose	7.87	17.95	39.49	4.08	19.8	7.87
D-Sorbitol	7.43	16.95	56.44	7.65	22.5	7.43
Galactose	4.11	9.39	65.82	27.48	20.6	4.11
Xylose	4.08	9.3	75.12	8.15	0	4.08
Ribose	3.49	7.96	83.08	3.33	10.3	3.49
Arabinose	1.7	3.88	86.96	3.4	0	1.7
Melibiose	1.18	2.68	89.64	6.7	7.6	1.18
Trehalose	0.98	2.23	91.87	4.15	2.2	0.98
c) Average dissimilarity = 52.84						
Group	Estuarine			Marine		
Sugars	Av. Diss	Contrib%	Cum.%	Av. Abund	Av. Abund	Diss/SD
Mannose	11.97	22.65	22.65	27.98	0	0.94
D-Sorbitol	8.86	16.77	39.42	3.42	22.5	5.54
Fructose	8.38	15.87	55.28	1.7	19.8	7.61
Melibiose	7.23	13.69	68.97	22.84	7.6	1.54
Galactose	2.96	5.61	74.58	14.16	20.6	1.66
Ribose	2.21	4.18	78.76	5.56	10.3	1.52
Arabinose	1.99	3.76	82.52	4.32	0	1.15
Lactose	1.76	3.33	85.86	9.12	5.3	2.15
Xylose	1.53	2.89	88.75	3.72	0	0.63
Inositol	1.21	2.3	91.04	3.76	1.2	1.58

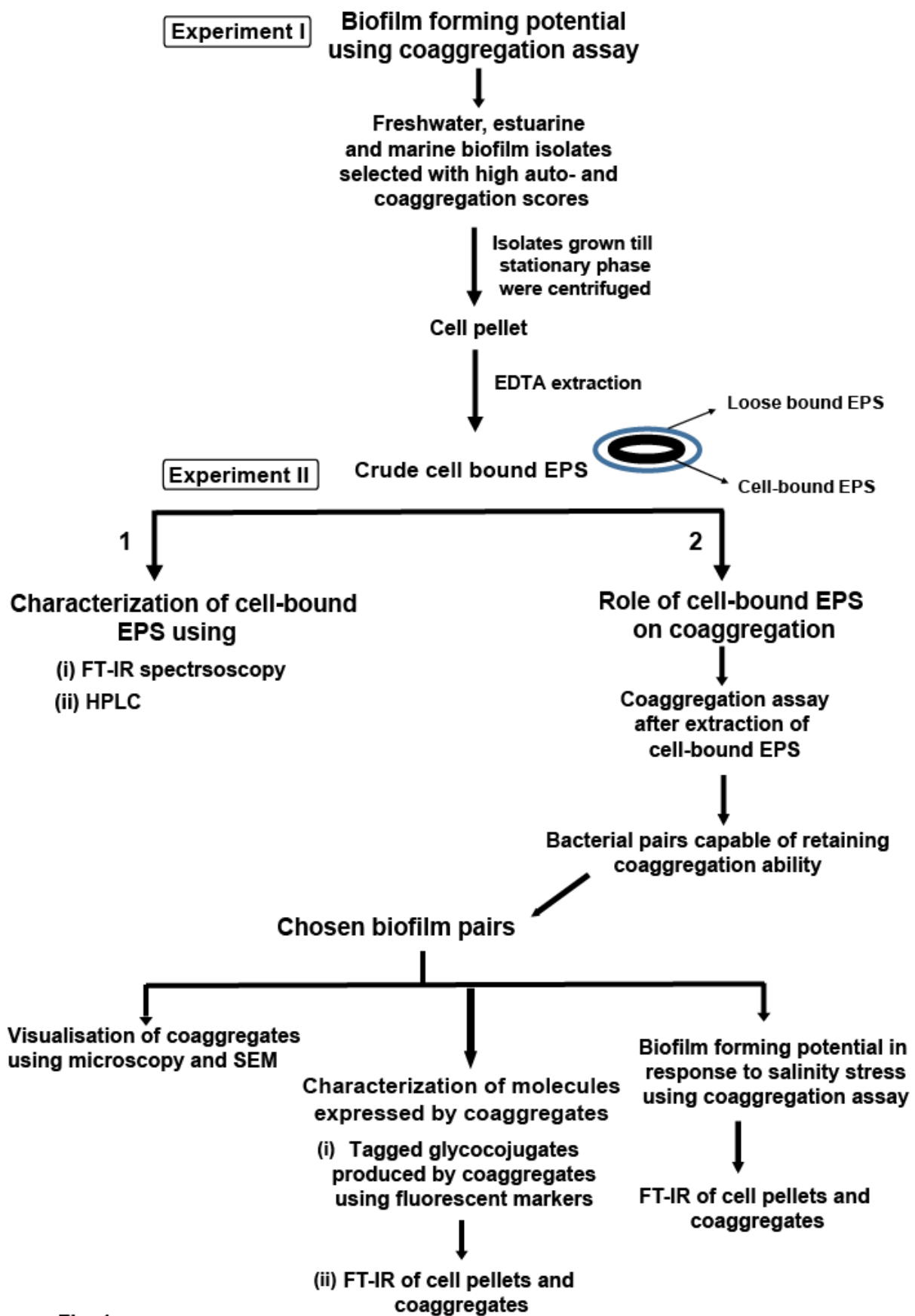


Fig. 1

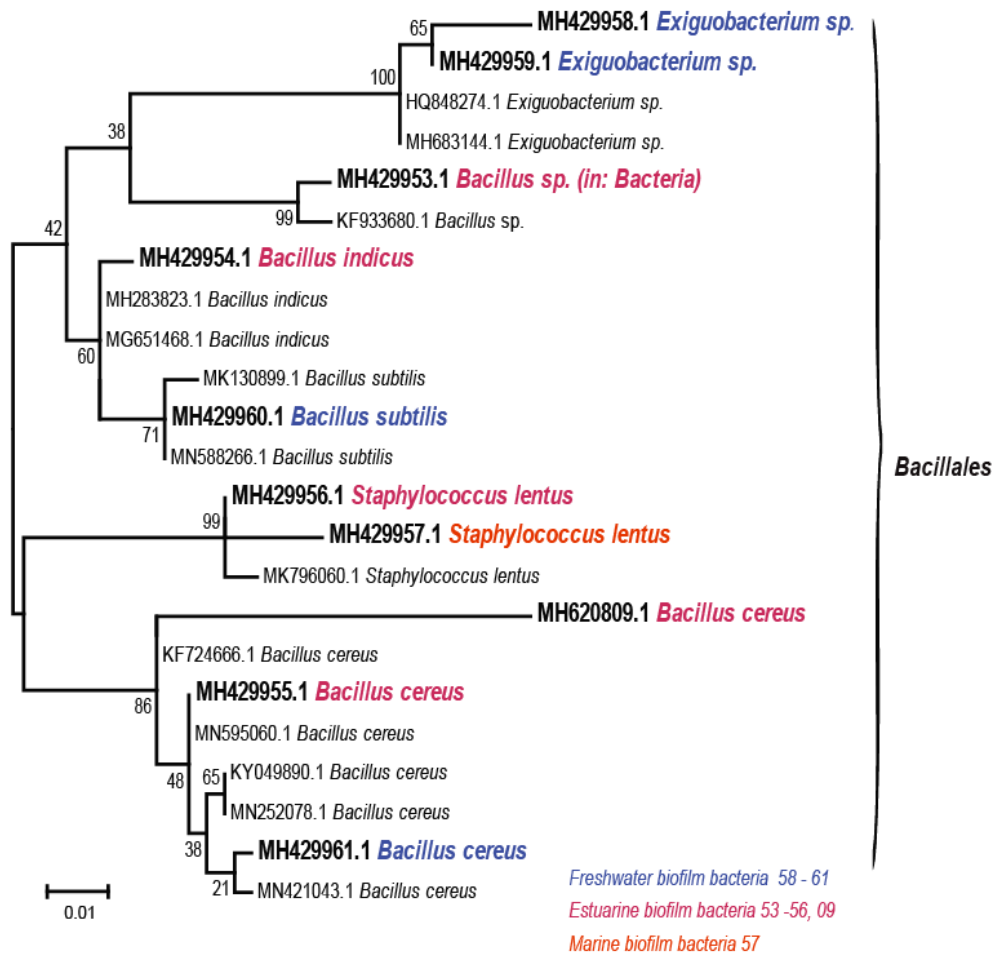


Fig. 2

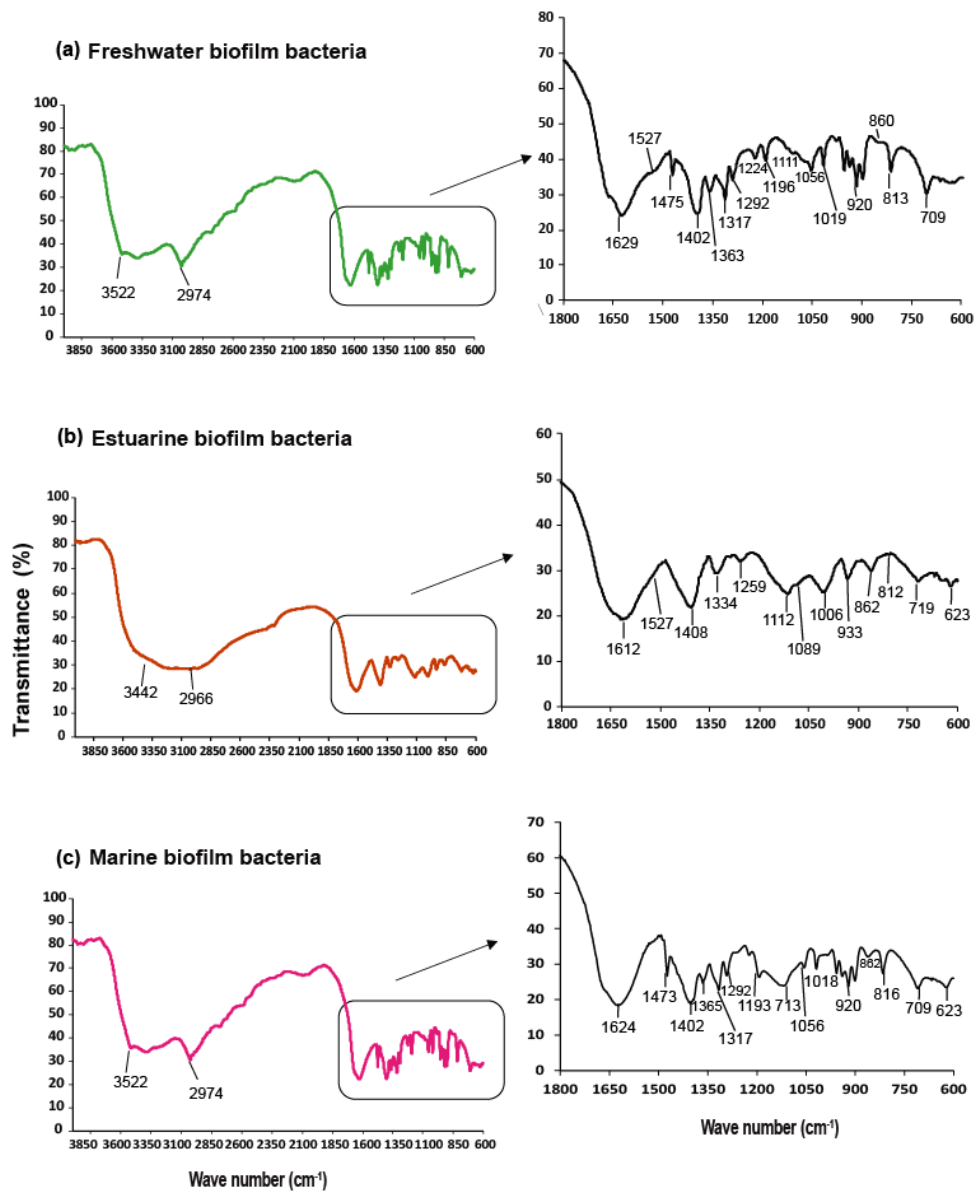
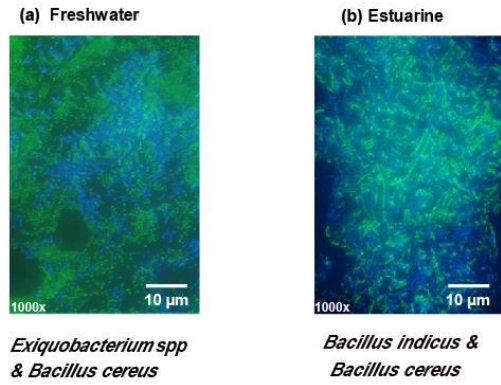


Fig. 3

Visualization of coaggregates using epifluorescence microscopy



SEM observation of coaggregates

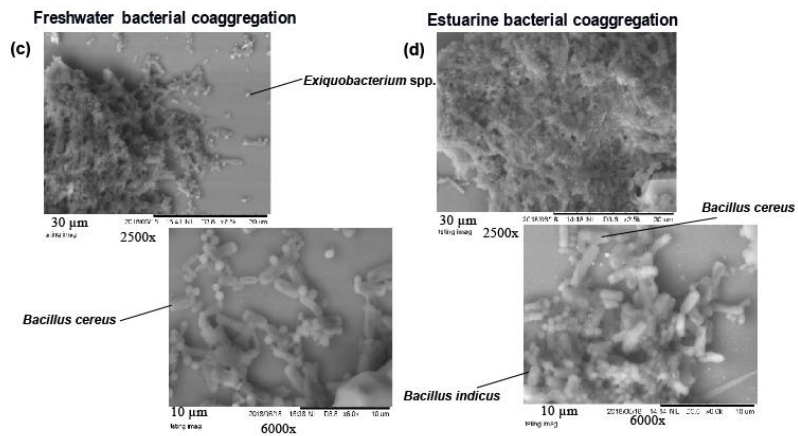


Fig. 4

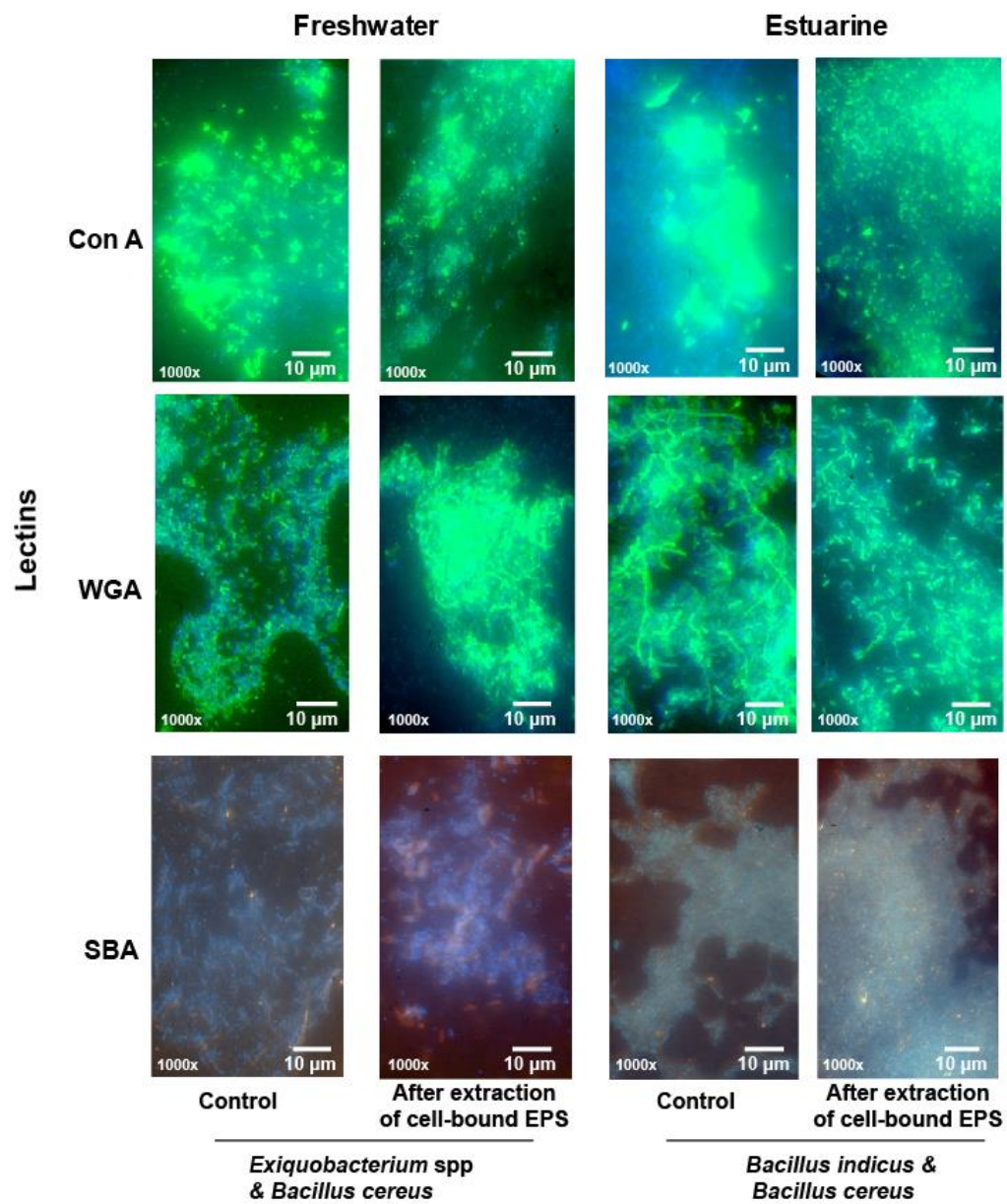
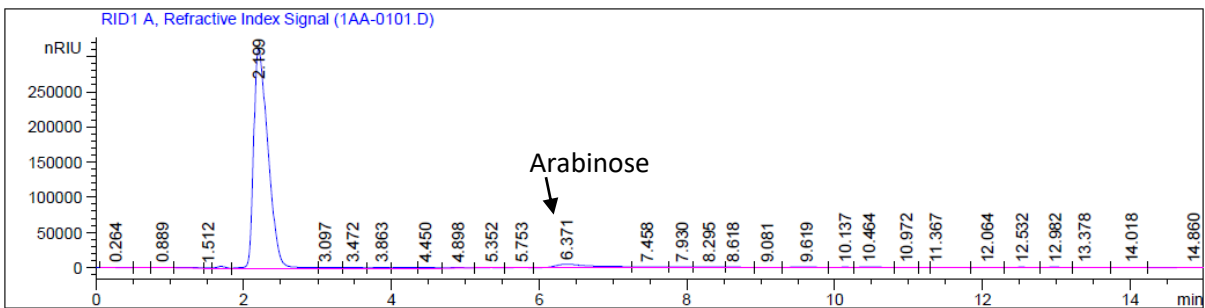
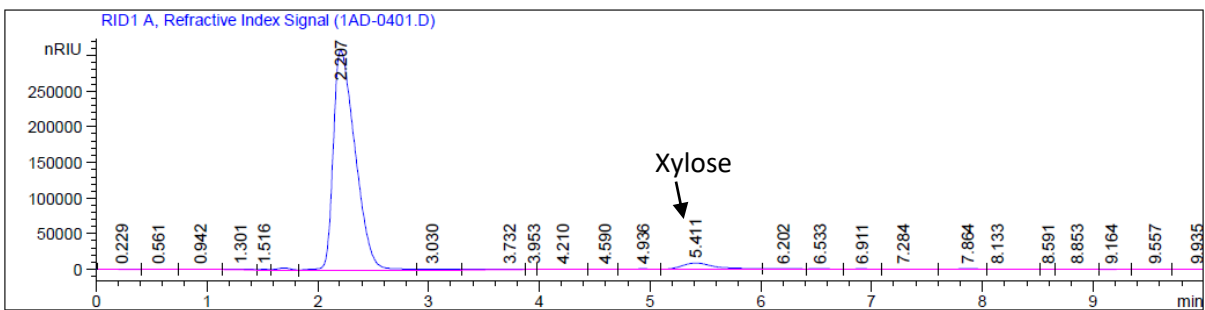
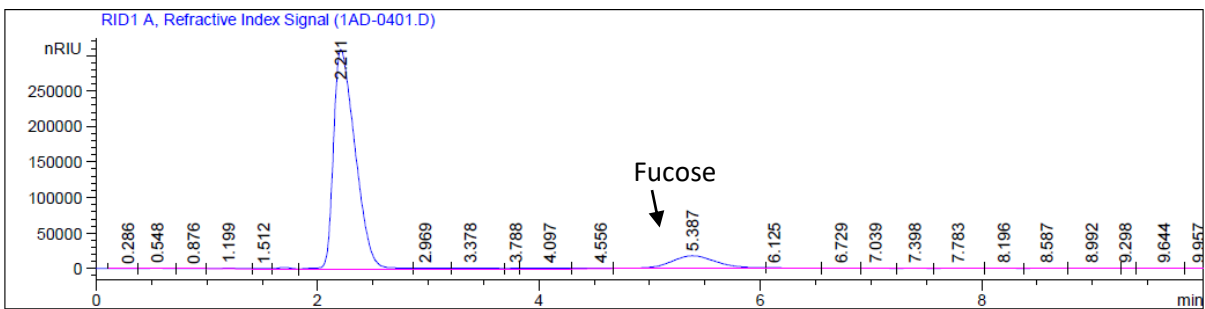
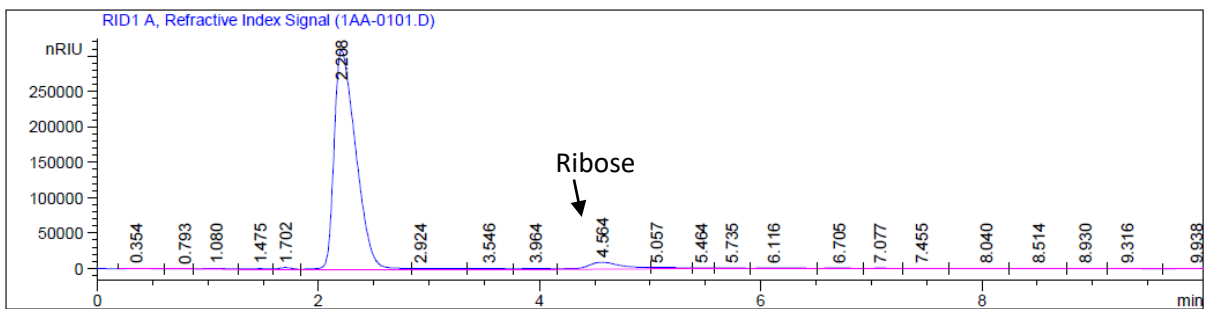
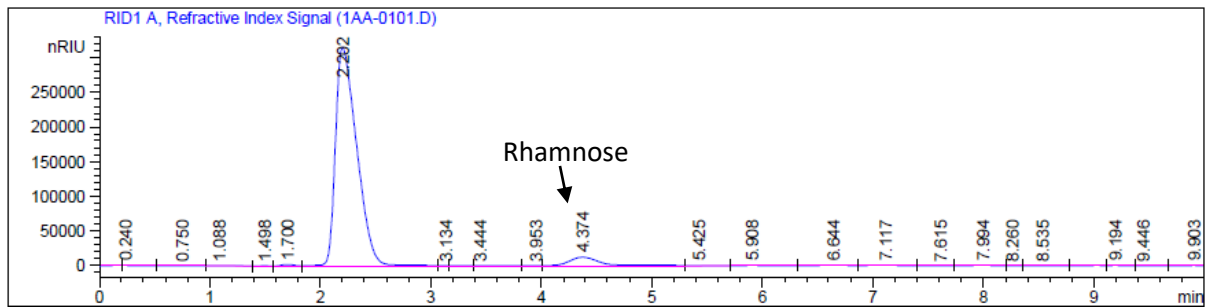
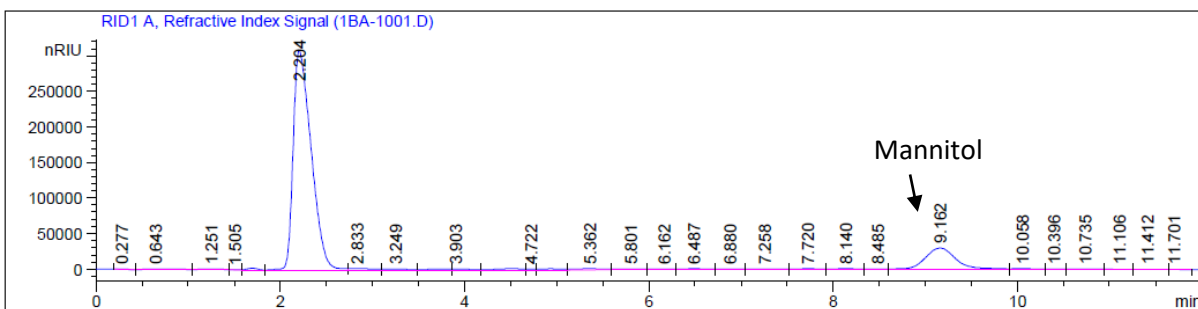
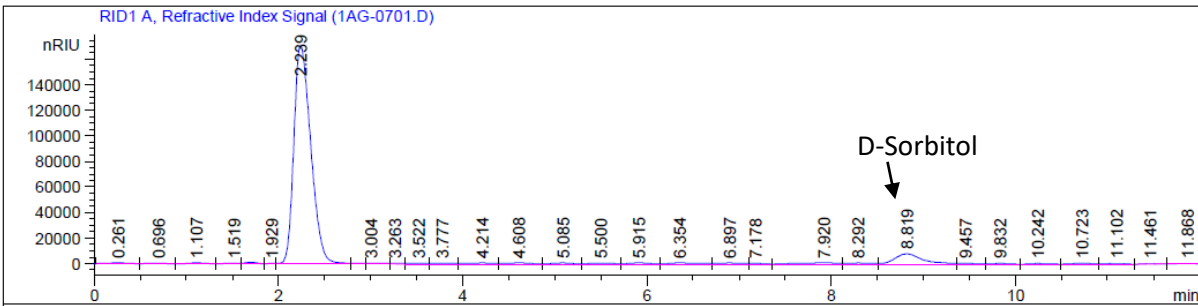
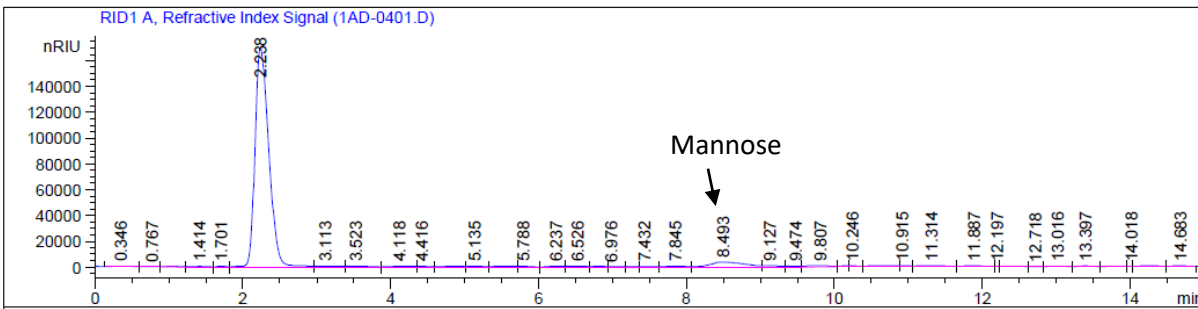
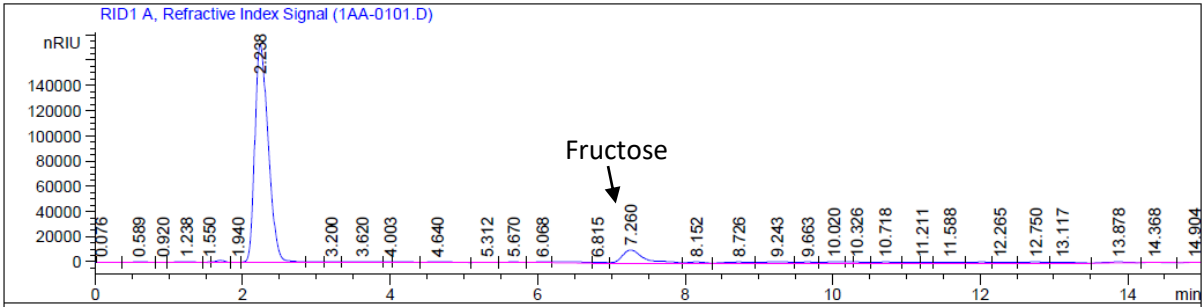
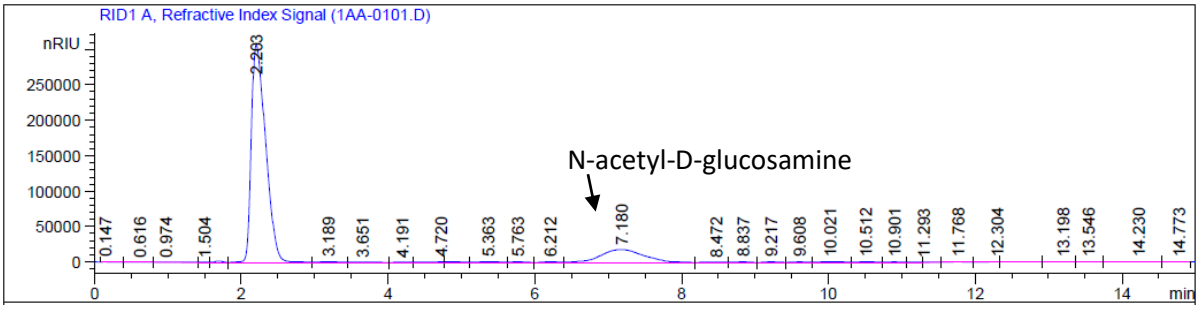
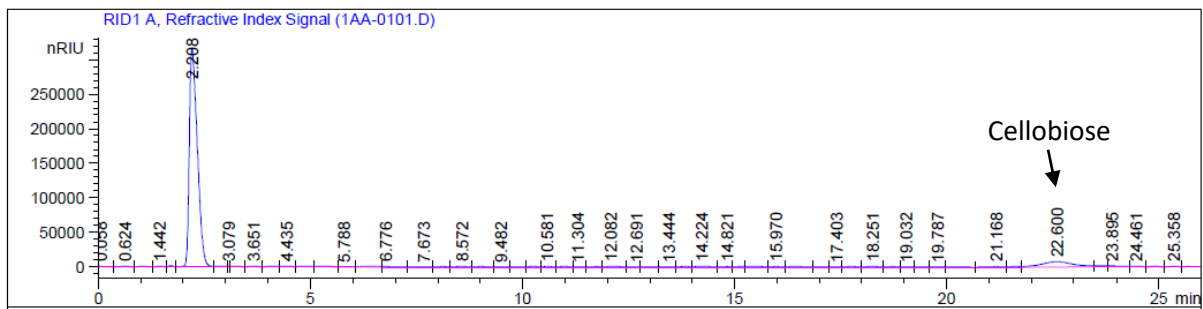
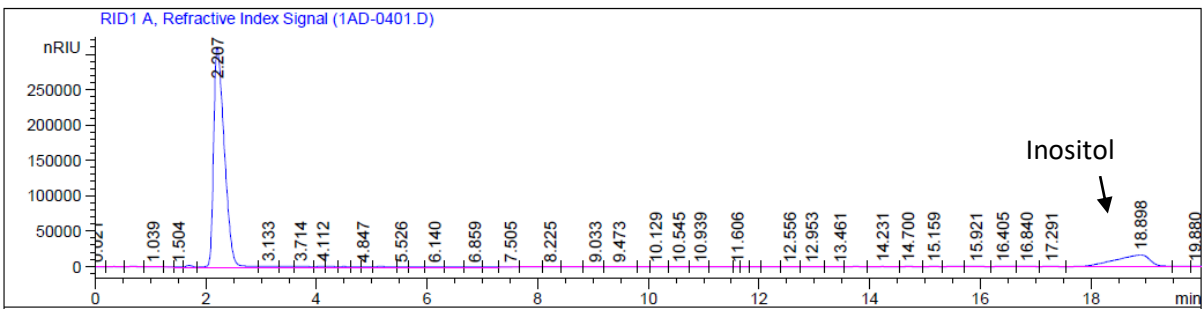
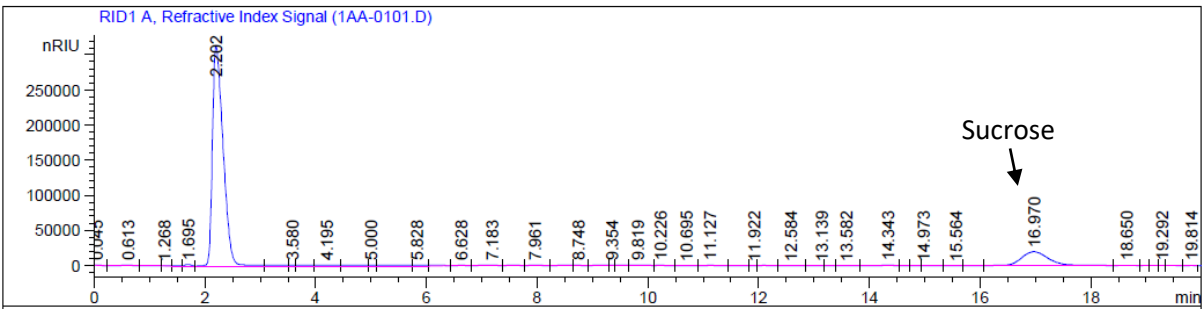
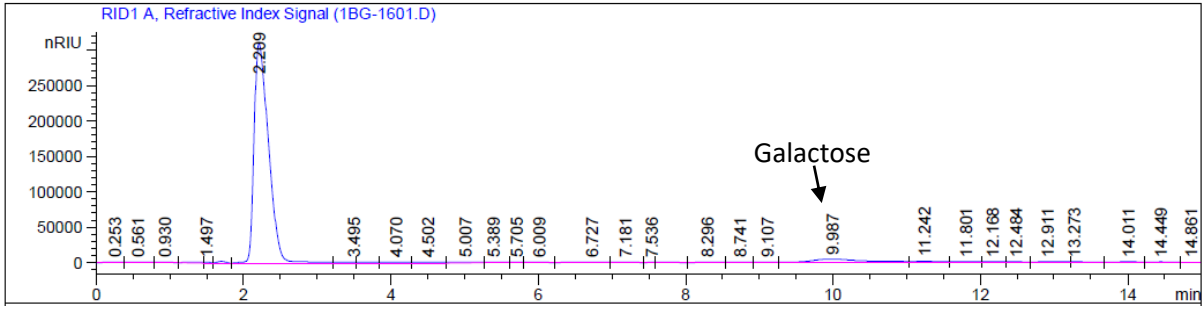
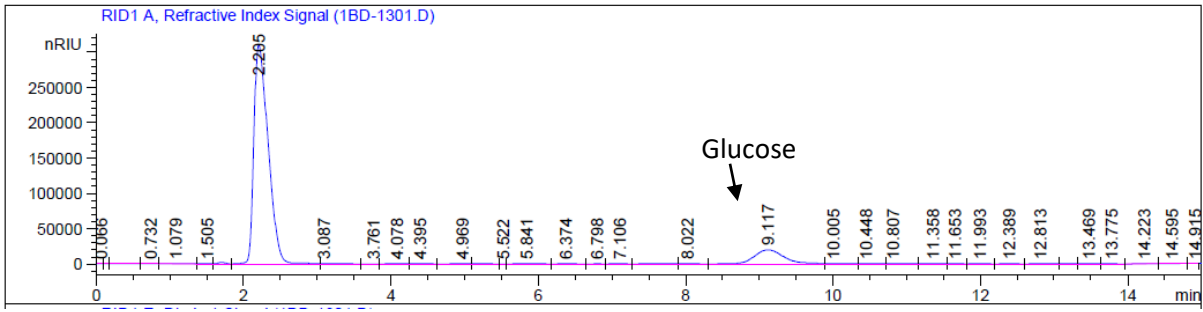


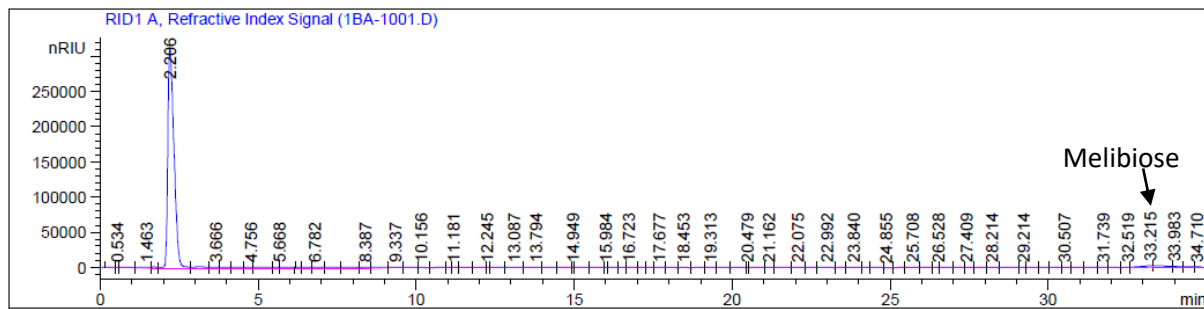
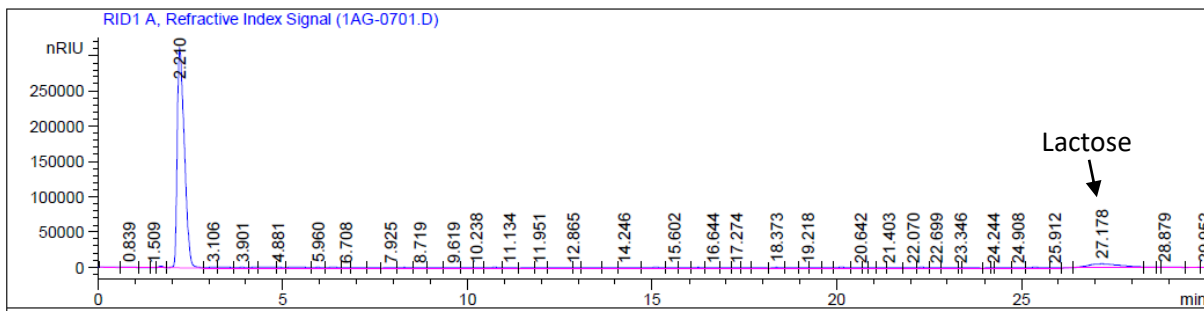
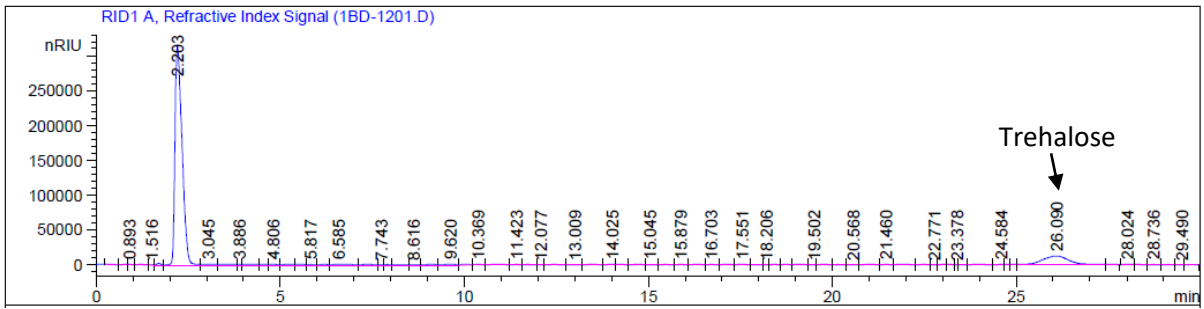
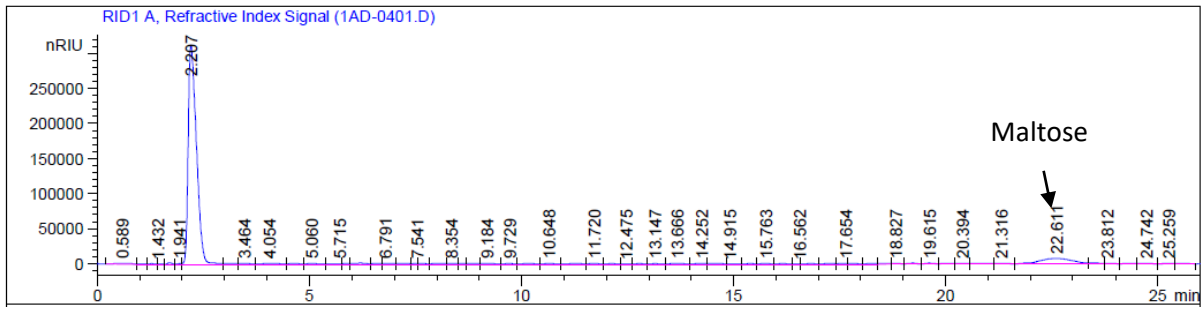
Fig. 5

Electronic supplementary material (ESM)









ESM_1a: Chromatograms of 19 sugar standards (Concentration: 10mg/ml)

		SUGARS	Retention Time (RT)
1	Monosaccharides	Rhamnose	4.374
2		Ribose	4.564
3		D Fucose	5.387
4		Xylose	5.411
5		Arabinose	6.371
6		N-acetyl-D-glucosamine	7.18
7		Fructose	7.26
8		Mannose	8.493
9		D- Sorbitol	8.819
10		Glucose	9.117
11		Mannitol	9.162
12		Galactose	9.987
13	Disaccharides	Sucrose	16.97
14		Inositol	18.898
15		Cellobiose	22.6
16		Maltose	22.611
17		Trehalose	26.09
18		Lactose	27.178
19		Melibiose	33.215

ESM_1b: Sugars standards with their retention times

(a)

Coaggregation scores Freshwater biofilm bacteria	1-2	1-3	1-4	1-5	1-6	1-7	1-8	1-9	
	2	2	2	3	2	3	4	3	
Total strains - 9 Selected - 4	2-3	2-4	2-5	2-6	2-7	2-8	2-9		
	3	3	3	3	3	4	3		
	3-4	3-5	3-6	3-7	3-8	3-9			
	3	3	2	3	4	3			
	4-5	4-6	4-7	4-8	4-9				
	3	2	3	4	3				
	5-6	5-7	5-8	5-9					
	3	4	4	3					
	6-7	6-8	6-9						
	2	3	2						
	7-8	7-9							
	4	4							
	8-9								
	4								
Strains	1	2	3	4	5	6	7	8	9
Autoaggregation scores	2	2	2	2	3	1	4	4	4
					F1		F2	F3	F4

F - Freshwater
E - Estuarine
M - Estuarine

(b)

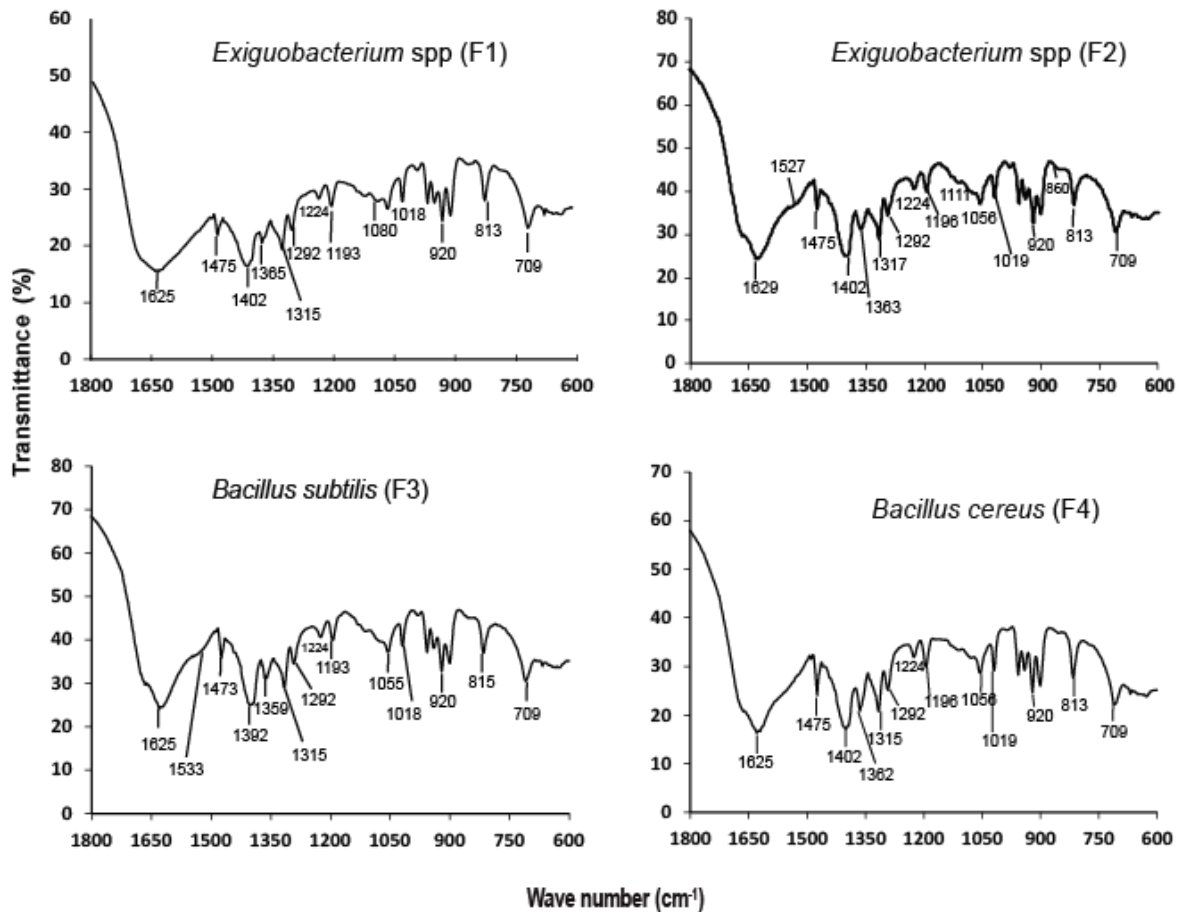
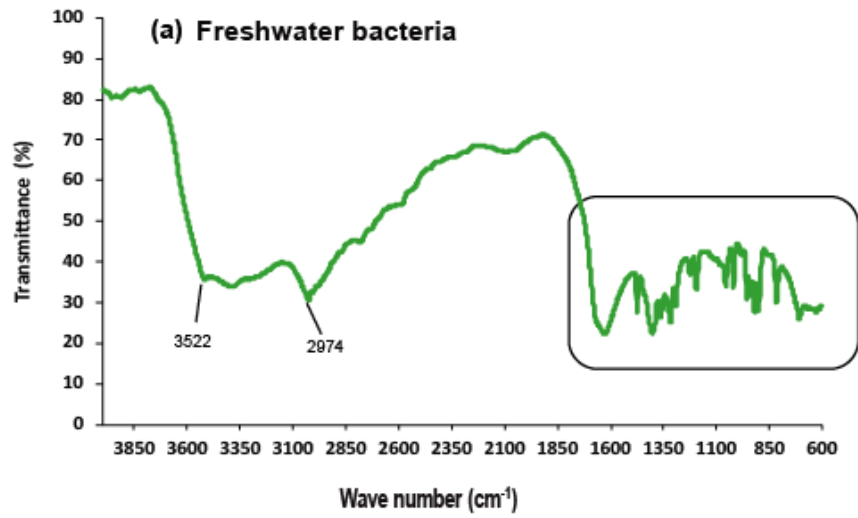
Coaggregation scores Estuarine biofilm bacteria	1-2	1-3	1-4	1-5	1-6	1-7	1-8	
	2	2	3	2	2	3	2	
Total strains - 8 Selected - 5	2-3	2-4	2-5	2-6	2-7	2-8		
	2	3	3	3	4	4		
	3-4	3-5	3-6	3-7	3-8			
	4	2	2	4	4			
	4-5	4-6	4-7	4-8				
	3	4	4	4				
	5-6	5-7	5-8					
	2	2	2					
	6-7	6-8						
	2	2						
	7-8							
	4							
Strains	1	2	3	4	5	6	7	8
Autoaggregation scores	2	3	4	4	2	4	4	4
			E1	E2		E3	E4	E5

(c)

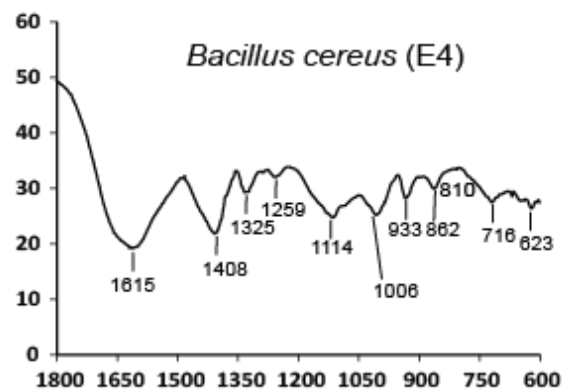
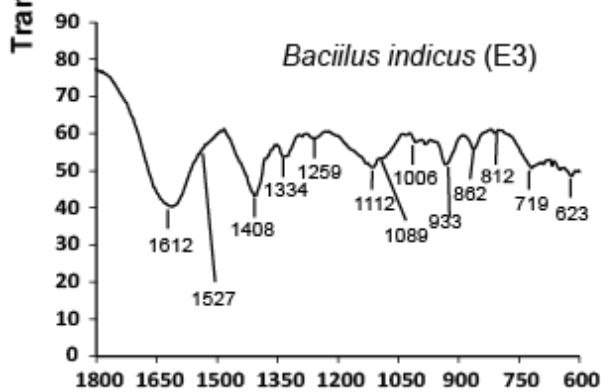
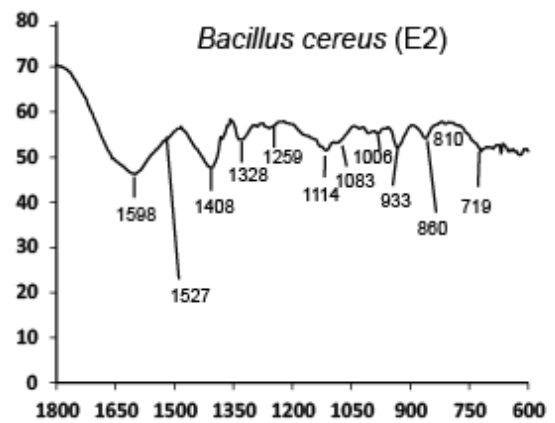
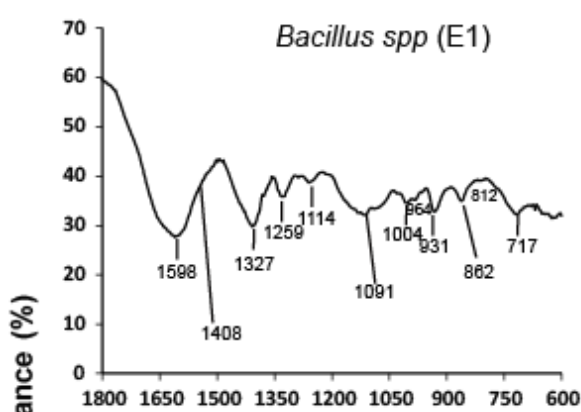
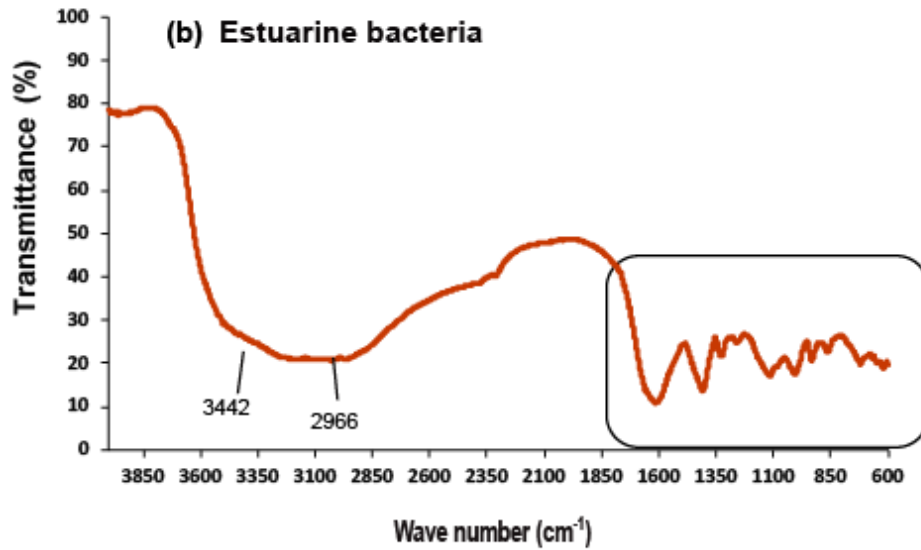
Coaggregation scores Marine biofilm bacteria	1-2	1-3	1-4	1-5	1-6	
	2	1	1	1	1	
Total strains - 6 Selected - 1	2-3	2-4	2-5	2-6		
	1	3	3	3		
	3-4	3-5	3-6			
	1	1	1			
	4-5	4-6				
	0	0				
	5-6					
	0					
Strains	1	2	3	4	5	6
Autoaggregation scores	1	3	1	1	1	1
		M1				

ESM_2

○ Selected strains for further characterisation

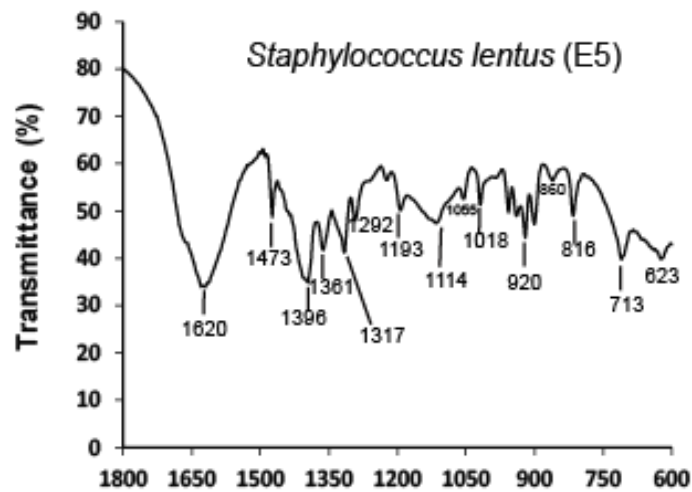
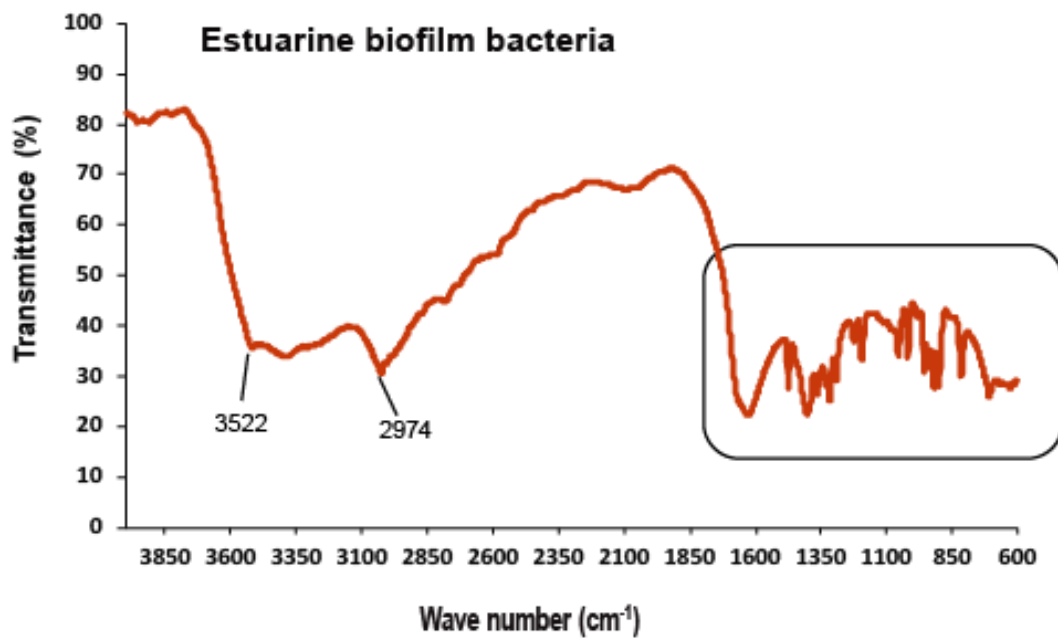


ESM_3a Fourier-transform infrared (FT-IR) spectra's of cell-bound EPS extracted from freshwater biofilm-forming bacteria. The freshwater bacterial EPS spectra is represented in green colour. The zoomed infra-red (1800 - 600 cm⁻¹) spectral section is shown in black colour. F= Freshwater.

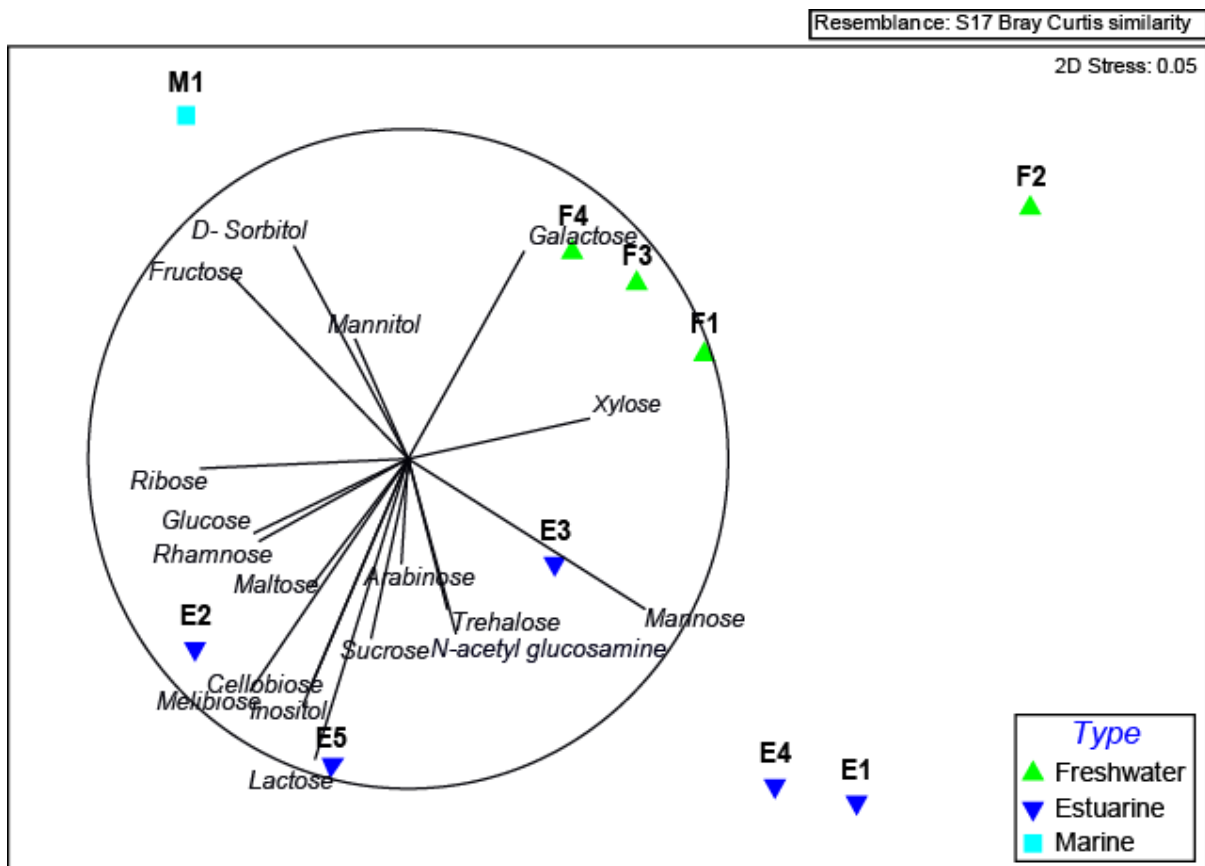


Wave number (cm⁻¹)

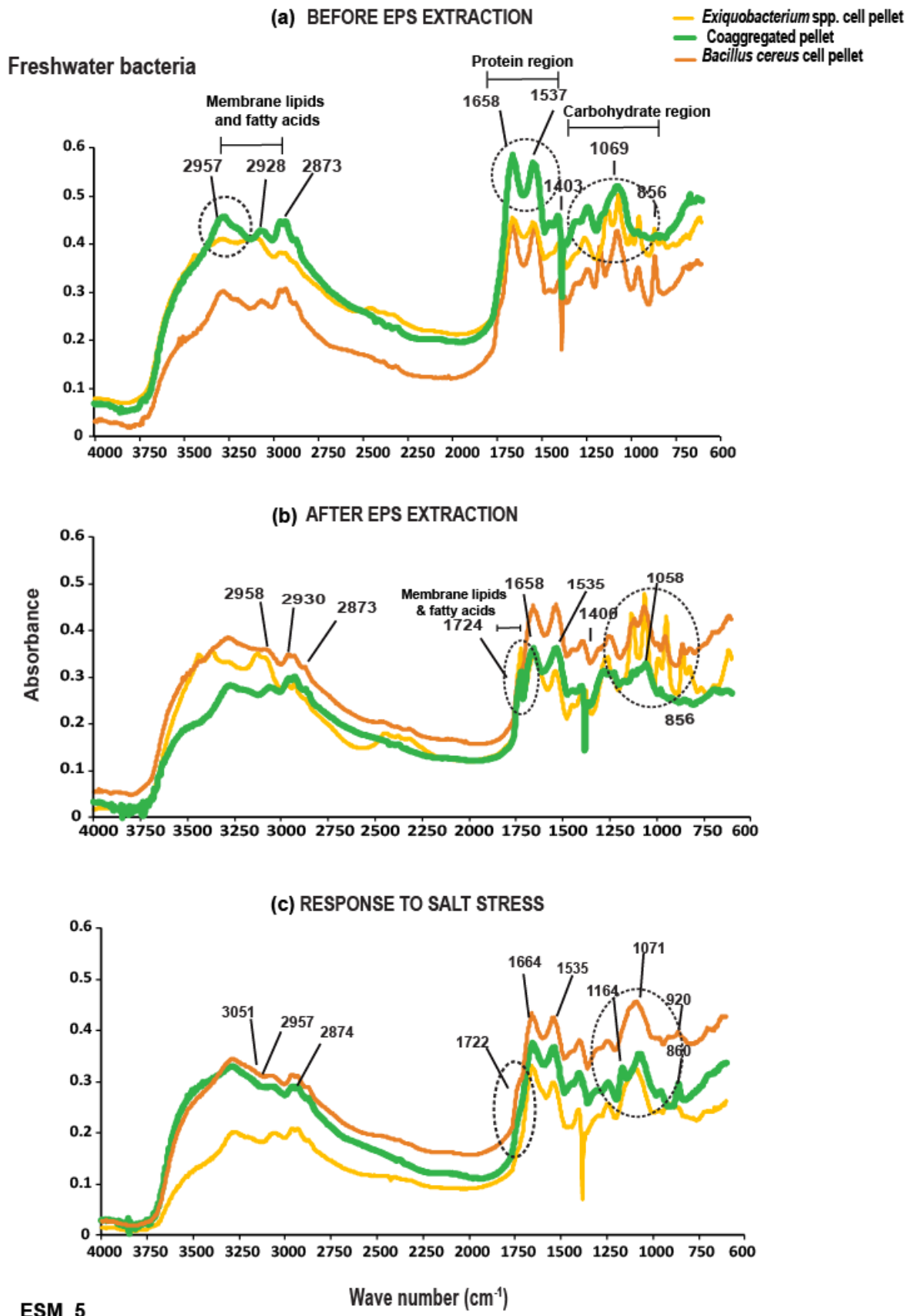
ESM_3b Fourier-transform infrared (FT-IR) spectra's of cell-bound EPS extracted from estuarine biofilm-forming bacteria. The estuarine bacterial EPS spectra in orange colour. The zoomed infra-red (1800 - 600 cm⁻¹) spectral section is shown in black colour. E = Estuarine. One of the estuarine (MH429956.1), showed a spectral pattern similar to the freshwater bacteria as shown below.



ESM_3c Fourier-transform infrared (FT-IR) spectra's of cell-bound EPS extracted from estuarine biofilm-forming bacteria depicting spectral pattern similar to the freshwater bacteria. The estuarine bacterial EPS spectra in orange colour. The zoomed infra-red (1800 - 600 cm⁻¹) spectral section is shown in black colour. E = Estuarine.



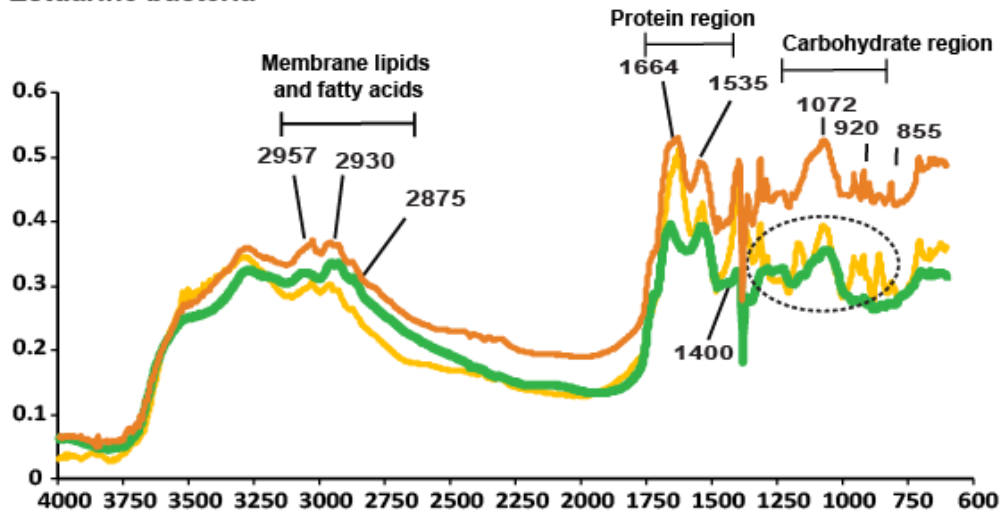
ESM_4



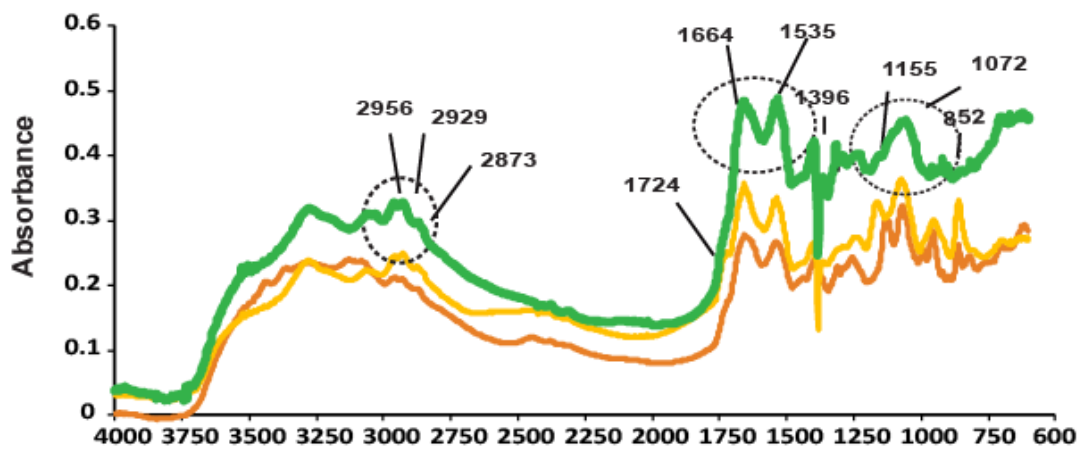
a) BEFORE EPS EXTRACTION

Estuarine bacteria

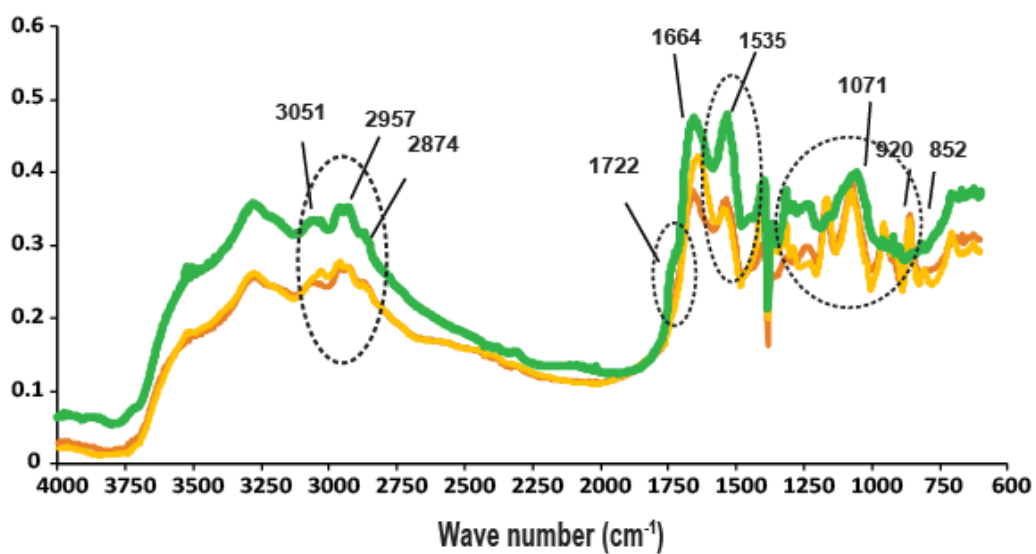
— *Bacillus cereus* cell pellet
 — Coaggregated pellet
 — *Bacillus indicus* cell pellet



b) AFTER EPS EXTRACTION



c) RESPONSE TO SALT STRESS



ESM_6